Criticality and the Chiral Phase Transition

Kritikalität und der chirale Phasenübergang

Bachelorarbeit im Fach Physik

vorgelegt von

Konstantin Otto

Betreuer und Erstbegutachter:

PD Dr. Bernd-Jochen Schaefer

Zweitbegutachter:

Prof. Dr. Christian Fischer

27. August 2014

Institut für Theoretische Physik
Justus-Liebig-Universität Gießen

JUSTUS-LIEBIG-
UNIVERSITÄT
GIESSEN

Contents

1 Introduction

In describing statistical processes and the microscopic interactions in particle physics, Quantum Field Theory has had a lot of success. Nevertheless, one still encounters problems attempting to describe strongly interacting matter. Due to the running of the strong coupling constant, perturbation theory only succeeds at small scales or high momenta. In order to produce physical results, a higher focus has been put upon the development of non-perturbative methods. One of them is the *functional renormalization group*. With the help of functional methods, the system is only regarded in a small momentum shell and a flow equation is obtained. This could, e.g., be the infinitesimal change of the partition function under an infinitesimal change of the regarded momentum. With the knowledge of the partition function at a certain scale, the system can be evolved until all fluctuations are included and the full partition function is obtained [1]. The *proper-time renormalization group* (PTRG) approximates this flow in a good fashion. In this work, the application of the PTRG to a quark-meson model is studied concerning critical behaviour and chiral phase transitions. Therefore, the flow equation, which is a partial differential equation, is expanded in a Taylor series. The ordinary differential equations obtained this way can be solved numerically.

2 Functional Methods in Quantum Field Theory

In the following section, the functional methods needed to derive the renormalization group flow equations will be briefly introduced. A functional $F[\varphi]$ on a space of functions maps each function $\varphi(x)$ to e.g. a scalar value. Thus, it is a function of a function and does not take a discrete amount of variables x_i, but rather a continuum of variables $\varphi(x),\ x \in \mathbb{R}$. A path integral in Quantum Field Theory is a functional integral, which is, for real scalar fields, defined as

$$\int \mathcal{D}\varphi\, F[\varphi] \equiv \lim_{n\to\infty} \int_{-\infty}^{\infty} \left(\prod_{i=1}^{n} \frac{\mathrm{d}\alpha_i}{\sqrt{2\pi}} \right) F(\alpha_1, ..., \alpha_n), \tag{1}$$

where $\varphi(x) = \sum_{i=1}^{\infty} \alpha_i\, u_i(x)$ is formed by a complete set of orthonormal functions [2]. All possible configurations of $\varphi(x)$ are included in this form, thus it makes sense that the partition function of a statistical population is a weighted functional integral:

$$Z[J] = \int \mathcal{D}\varphi\, \mathrm{e}^{-S[\varphi] + \int_x J(x)\varphi(x)}. \tag{2}$$

$J(x)$ is an external source term and $S[\varphi]$ is the action

$$S = \int \mathrm{d}^4x\, \mathscr{L}. \tag{3}$$

It is the four-dimensional integral of the Lagrangian density. For Quantum Chromodynamics, it reads

$$\mathscr{L} = \mathscr{L}_{\mathrm{G}'} + \mathscr{L}_{\mathrm{g}} + \mathscr{L}_{\mathrm{q}}, \tag{4}$$

where

$$\mathscr{L}_{\mathrm{G}'} = -\frac{1}{4} G_{i\mu\nu}(x) G_i^{\mu\nu}(x) - \frac{1}{2} \left(\partial_\mu A_i^\mu(x)\right)^2 \tag{5}$$

describes the interaction of the gluon fields $A_i^\mu(x)$. Depending on the gauge being used, a ghost term must be introduced:

$$\mathscr{L}_\mathrm{g} = \partial_\mu \eta_i(x)\,[\partial^\mu \tilde{\eta}_i(x) + g_s\, f_{ijk}\, \tilde{\eta}_j(x)\, A_k^\mu(x)] \tag{6}$$

η and $\tilde{\eta}$ are virtual anti-commuting (Grassmann) fields that interact with the gluons. The quarks are included by

$$\mathscr{L}_\mathrm{q} = \overline{\psi}_a(x)\,[\mathrm{i}\not{D}_{ab} - \delta_{ab} m]\,\psi_b(x), \tag{7}$$

with

$$\not{D}_{ab} = \gamma_\mu \left(\delta_{ab}\partial^\mu + \frac{1}{2}\,\mathrm{i}\, g_s (\lambda_j)_{ab}\, A_j^\mu(x) \right). \tag{8}$$

Note that the partition function is expressed in four-dimensional Euclidean metric, that can be obtained from the Minkowski space-time metric by a Wick rotation $t \to -\mathrm{i}\tau$. $Z[J]$ also acts as a generating functional for the n-point correlators:

$$\langle \varphi(x_1) \dots \varphi(x_n) \rangle = \frac{1}{Z[0]}\, \frac{\delta^n Z[J]}{\delta J(x_1) \dots \delta J(x_n)}\bigg|_{J=0} = \frac{1}{Z[0]} \int \mathcal{D}\varphi\, \varphi(x_1) \dots \varphi(x_n)\, \mathrm{e}^{-S[\varphi]} \tag{9}$$

Its logarithm,

$$W[J] := \ln Z[J], \tag{10}$$

is the generating functional for connected correlators, such as the connected Green function

$$G(x,y) = \frac{\delta^2 W[J]}{\delta J(x) \delta J(y)} = \langle \varphi(x)\varphi(y) \rangle - \langle \varphi(x) \rangle \langle \varphi(y) \rangle. \tag{11}$$

The classical field can be obtained from the generating functional as well:

$$\phi(x) = \frac{\delta W[J]}{\delta J(x)} = \langle \varphi(x) \rangle. \tag{12}$$

Furthermore, we define the *effective action* as the Legendre transformation of $W[J]$:

$$\Gamma[\phi] := \sup_J \left(\int J\phi - W[J] \right). \tag{13}$$

Taking the supremum ensures that the functional is convex [1]. We are now able to find the *quantum equation of motion*:

$$\frac{\delta \Gamma[\phi]}{\delta \phi(x)} = J(x) + \int_y \frac{\delta J(y)}{\delta \phi(x)} \phi(y) - \int_y \frac{\delta W[J]}{\delta J(y)} \frac{\delta J(y)}{\delta \phi(x)} \overset{(12)}{=} J(x). \tag{14}$$

3 The Functional Renormalization Group

The derivation of the functional renormalization group (FRG) roughly follows the steps performed in [1]. The strategy behind the functional renormalization group approach follows Wilson's idea of looking at the problem in statistical physics only at a certain scale and then using the known scale dependence to evaluate the system from a starting point to the desired end point. In practice, this is done by adding a scale dependent action term $\Delta S_k[\varphi]$ in the exponential of the generating functional (eq. (2)):

$$Z_k[J] = \int \mathcal{D}\varphi \, \mathrm{e}^{-S[\varphi]-\Delta S_k[\varphi]+\int_x J(x)\varphi(x)}, \tag{15}$$

which reads

$$\Delta S_k[\varphi] = \frac{1}{2}\int \frac{\mathrm{d}^d q}{(2\pi)^d}\, \varphi(-q) R_k(q)\varphi(q). \tag{16}$$

$R_k(q)$ is a regulator function providing an IR regularization. It guarantees that only small momentum shells around k are considered in the evaluation of the functional differential equation (which we will find at the end of this section) towards $k = 0$. At this point, all the fluctuations are taken into account and the original action has to be restored. This implies certain requirements for the regulator. Firstly,

$$\lim_{q^2/k^2\to 0} R_k(q) > 0 \tag{17}$$

ensures the IR regularization. Often, $R_k \sim k^2$ for $q^2 \ll k^2$ is used, which gives evidence that ΔS_k serves as a dynamic mass term [1]. Secondly,

$$\lim_{k^2/q^2\to 0} R_k(q) = 0 \tag{18}$$

leads to the full (effective) action at $k = 0$. The last condition is

$$\lim_{k^2\to\Lambda} R_k(q) \to \infty, \tag{19}$$

which gives the bare action $\Gamma_k \xrightarrow{k\to\Lambda} S_{(\mathrm{bare})}$ at the UV cutoff Λ. Γ_k is now k-dependent, being called the *effective average action*. Although the trajectory taken by the effective average action in theory space depends on the regulator function, the conditions introduced above make sure that the start point $\Gamma_{k=\Lambda} = S_{(\mathrm{bare})}$ and the end point at $\Gamma_{k=0} = \Gamma$ always stay the same. Additionally, we slightly change the definition of Γ_k by subtracting ΔS_k:

$$\Gamma_k[\phi] = \sup_J \left(\int_x J(x)\phi(x) - W_k[J] \right) - \Delta S_k[\phi] \tag{20}$$

It is now possible to show that Γ_k converges against the classical action at the UV cutoff. Therefore, we examine the exponential of the effective average action:

$$\mathrm{e}^{-\Gamma_k[\phi]} = \mathrm{e}^{W_k[J]-\int_x J(x)\phi(x)+\Delta S_k[\phi]} = \int \mathcal{D}\varphi \, \mathrm{e}^{-S[\varphi]+\int_x J(x)(\varphi(x)-\phi(x))-\Delta S_k[\varphi]+\Delta S_k[\phi]}. \tag{21}$$

Using the substitution $\varphi' = \varphi - \phi$ and the definition of ΔS_k, we get

$$\mathrm{e}^{-\Gamma_k[\phi]} = \int \mathcal{D}\varphi \, \mathrm{e}^{-S[\varphi'+\phi]+\int_x J(x)\varphi'(x)-\frac{1}{2}\int \frac{\mathrm{d}^d p}{(2\pi)^d} R_k(p)(\varphi'(-p)\varphi'(p)+\varphi'(-p)\phi(p)+\phi(-p)\varphi'(p))} \tag{22}$$

For $R_k \to \infty$, the term $\exp\left(\int_p \varphi'(-p) R_k \varphi'(p)\right)$ acts as a delta functional $\delta[\phi]$ [3], thus leading to

$$\mathrm{e}^{-\Gamma_k[\phi]} \to \mathrm{e}^{-S[\phi]}. \tag{23}$$

Following the renormalization group idea, we can now perform a derivation of $W_k[J]$ with respect to k. We will however use the convention [1]

$$t = \ln \frac{k}{\Lambda}, \qquad \partial_t = k \frac{\mathrm{d}}{\mathrm{d}k}, \tag{24}$$

and the definition of ΔS_k to obtain

$$\partial_t W_k[J] = \partial_t \ln Z_k[J] = -\frac{1}{2} \int \frac{\mathrm{d}^d q}{(2\pi)^d}\, \partial_t R_k(q)\, G_k(q) + \partial_t \Delta S_k[\phi], \tag{25}$$

where $G(q)$ is the Fourier transform of the connected two-point Green function (11). $\phi(x) = \langle \varphi(x) \rangle$ denotes the expectation value as defined in (12). The derivative of $\Gamma_k[\phi]$ delivers a modified quantum equation of motion (compare to equation (14)):

$$\frac{\delta \Gamma_k[\phi]}{\delta \phi(x)} = J(x) - R_k(x)\phi(x). \tag{26}$$

Here, the Fourier transformed regulator term for real scalar fields is used. This helps us to find the relation

$$\frac{\delta J(x)}{\delta \phi(y)} = \frac{\delta^2 \Gamma_k[\phi]}{\delta \phi(x) \delta \phi(y)} + R_k(x,y), \tag{27}$$

with $R_k(x,y) = R_k(x)\delta(x-y)$. The second relation we require is found by expressing the classical field ϕ as the functional derivative of $W_k[J]$ (compare to (12)). Now, the connected Green function (in coordinate space) can be reproduced:

$$\frac{\delta \phi(y)}{\delta J(z)} = \frac{\delta^2 W_k[J]}{\delta J(z) \delta J(y)} \equiv G_k(y-z) \tag{28}$$

Combining these two relations, (27) and (28), one can write the delta function as

$$\delta(x-z) = \int_y \frac{\delta J(x)}{\delta \phi(y)} \frac{\delta \phi(y)}{\delta J(z)} = \int_y \left(\frac{\delta^2 \Gamma_k[\phi]}{\delta \phi(x) \delta \phi(y)} + R_k(x,y) \right) G_k(y,z) \tag{29}$$

Writing the nth functional derivative of $\Gamma_k[\phi]$ as an uppercase index in parenthesis, one finds

$$\mathbb{1} = (\Gamma_k^{(2)} + R_k)\, G_k, \tag{30}$$

which is to be interpreted as an operator notation, with the multiplication being a matrix multiplication extended to continuous coordinate space. The actual flow equation is obtained by inserting the results from eq. (25) and (30) into the t-derivative of the effective average action (20). Note that this is a partial derivative, meaning the classical field ϕ is kept independent from the scaling factor. Necessarily, the source $J(x)$ has to be k-dependent, as the relation (12) still holds. This means that additionally to the partial derivative $\partial_t W_k[J]$, also the t-derivative of $J(x)$ in $W_k[J]$ must be taken into account:

$$\mathrm{d}_t W_k[J] = \partial_t W_k[J] + \int_x \frac{\delta W_k[J]}{\delta J(x)}\, \partial_t J(x) = \partial_t W_k[J] + \int_x \phi(x)\, \partial_t J(x), \tag{31}$$

which finally renders the functional renormalization group (FRG) flow equation:

$$\begin{aligned}\partial_t \Gamma_k[\phi] &= -\partial_t W_k[J] - \int_x \phi(x)\,\partial_t J(x) + \int_x \phi(x)\,\partial_t J(x) - \partial_t \Delta S_k[\phi] \\ &= \frac{1}{2}\int \frac{\mathrm{d}^d q}{(2\pi)^d}\,\partial_t R_k(q)\,G_k(q) = \frac{1}{2}\mathrm{Tr}\left[\partial_t R_k\left(\Gamma_k^{(2)}[\phi] + R_k\right)^{-1}\right].\end{aligned} \tag{32}$$

4 The Proper-Time Renormalization Group

In order to derive the *proper-time renormalization group* (PTRG) flow equation, one applies a *Schwinger proper-time regularization* [4] to the one-loop expansion of the effective action

$$\Gamma^{1-\mathrm{loop}}[\phi] = S[\phi] + \frac{1}{2}\mathrm{Tr}\ln S^{(2)}[\phi], \tag{33}$$

where we used the same notation as before:

$$S^{(2)}[\phi] = \frac{\delta^2 S[\phi]}{\delta\phi\delta\phi}. \tag{34}$$

The goal is to achieve a regularization of the logarithm [5]. At first, the *Schwinger proper-time representation* for an elliptic operator O is introduced:

$$O^{-1} = \lim_{\Lambda\to\infty}\int_{1/\Lambda^2}^{\infty} \mathrm{d}\tau\,\mathrm{e}^{-\tau O}. \tag{35}$$

An integration of both sides with respect to the operator and a subsequent tracing gives

$$\mathrm{Tr}(\ln O - \ln O_0) = -\int_0^\infty \frac{\mathrm{d}\tau}{\tau}\,f(\tau,\Lambda^2)\,\mathrm{Tr}\left(\mathrm{e}^{-\tau O} - \mathrm{e}^{-\tau O_0}\right), \tag{36}$$

where the UV regularization has been dragged into the integral by the function $f(\tau,\Lambda^2)$ with the property

$$\lim_{\tau\to 0} f(\tau,\Lambda^2) = 0. \tag{37}$$

This makes sure that the regularized integral stays finite. For an IR regularization, which will eventually deliver the flow equation, one just gives the regulator an additional k-dependence and opposes the condition

$$\lim_{\tau\to\infty} f_{k\neq 0}(\tau,\Lambda^2) = 0. \tag{38}$$

As the original physics have to be recovered in the limit $k = 0$, the conditions

$$\lim_{\Lambda\to\infty} f_{k=0}(\tau,\Lambda^2) = 1, \qquad \lim_{\tau\to\infty} f_{k=0}(\tau,\Lambda^2) = 1 \tag{39}$$

have to be fulfilled by the regulator function as well. In case the IR cutoff k and the UV cutoff Λ are the same, all fluctuations are neglected and the regulator has to become 0:

$$\lim_{k\to\Lambda} f_k(\tau,\Lambda^2) = 0. \tag{40}$$

Now, the regularized logarithm (36) can be inserted into one-loop expansion of the effective action (33):

$$\Gamma_k[\phi] = S[\phi] - \frac{1}{2}\int_0^\infty \frac{\mathrm{d}\tau}{\tau}\, f_k(\tau,\Lambda^2)\,\mathrm{Tr}\,\mathrm{e}^{-\tau\, S^{(2)}[\phi]} \tag{41}$$

Just like in the derivation of the FRG flow equation, the result is obtained by a derivation with respect to the scale variable $t = \ln(k/\Lambda)$:

$$\partial_t\Gamma_k[\phi] = -\frac{1}{2}\int_0^\infty \frac{\mathrm{d}\tau}{\tau}\, \partial_t f_k(\tau,\Lambda^2)\,\mathrm{Tr}\,\mathrm{e}^{-\tau\, S^{(2)}[\phi]}. \tag{42}$$

This is not a full functional differential equation for Γ_k yet. In the last step, the *renormalization group improvement* is applied by replacing $S^{(2)}[\phi]$ with the second functional derivative of the full effective average action, delivering the required differential equation [6, 7]:

$$\partial_t\Gamma_k[\phi] = -\frac{1}{2}\int_0^\infty \frac{\mathrm{d}\tau}{\tau}\, (\partial_t f_k(\tau,\Lambda^2))\,\mathrm{Tr}\,\mathrm{e}^{-\tau\, \Gamma_k^{(2)}[\phi]}. \tag{43}$$

Note that the derivative with respect to t still only affects the regulator function, as the classical action has been replaced with the effective average action thereafter.

5 The Quark-Meson Model

The quark-meson (QM) model can be described as an effective field theory. Its Lagrangian reads [8]

$$\mathscr{L}_{\mathrm{QM}} = \overline{q}\,(\mathrm{i}\partial\!\!\!/ - g\,(\sigma + \mathrm{i}\,\gamma_5\,\vec{\tau}\vec{\pi}))\,q + \frac{1}{2}\,(\partial_\mu\sigma)^2 + \frac{1}{2}\,(\partial_\mu\vec{\pi})^2 - U(\sigma,\vec{\pi}), \tag{44}$$

where the mesonic potential $U(\sigma,\vec{\pi})$ is characterized by

$$U(\sigma,\vec{\pi}) = \frac{\lambda}{4}(\sigma^2 + \vec{\pi}^2 - v^2)^2 - c\sigma. \tag{45}$$

Comparing the Lagrangian density with equation (4), one can see that any gluon interactions are neglected. Instead, a quark-meson Yukawa interaction and a mesonic potential have been added. This is due to the fact that the QM model shall describe QCD at the *compositeness scale* k_ϕ of about 1 GeV and below, where quarks and gluons compose into mesons. For higher energies, perturbation theory can be used, because then the coupling constant g_s is small enough. Between k_ϕ and the *chiral symmetry breaking scale* k_χ, which will be elaborated later, the system's dynamics are governed mainly by quark-meson interactions through the strong Yukawa coupling g. At the *confinement scale* k_{QCD} of about 200 MeV, quark confinement occurs and additional bound states form, which are not described in this model. However, the constituent quarks, having continually increased their mass since $k = k_\chi$, decouple from the meson dynamics. As we will later see, massive particles do not contribute as much to the flow equation. This justifies the usage of the QM model to solely describe the mesons up to the IR [6].

The quark fields q and $\overline{q}$ include two flavors, up- and down-quarks. The current quark

masses are set 0 in good approximation to the light quarks. The scalar σ field and the three pseudoscalar π fields can be summed up in a 4-vector $\phi = (\sigma, \vec{\pi})$ with $\langle\phi\rangle = \langle\sigma\rangle$ (since the expectation value of a pseudoscalar field is 0). Now the term $-c\sigma$ in the meson potential acts as an explicit chiral symmetry breaking term. If $c = 0$, the effective action Γ is invariant under global chiral $SU(2)_L \times SU(2)_R$ symmetry transformations [6]. The quark masses and the expectation value of the meson fields $\langle\phi\rangle$ are 0. As we will later see, this system experiences a spontaneous symmetry breaking at k_χ. One direction in ϕ is then distinguished and the expectation value $\langle\phi\rangle = \langle\sigma\rangle$ becomes non-vanishing. This comes with the existence of three massless Goldstone bosons, the pions. To account for the finite pion mass, which results from the difference of the up- and down-quark-masses that break the symmetry and which is neglected here, the explicit symmetry breaking term is introduced. If $c > 0$, the symmetry is broken right from the beginning, which implicates a finite quark mass $m_q = g\,\langle\sigma\rangle$ (compare to the mass term in the Lagrangian, (44)). Note that in the following evaluation, using the proper-time renormalization group flow equation, the running of the Yukawa coupling g is neglected. The parameter is chosen so that $m_q = 300$ MeV holds for $k \to 0$. c is considered to be scale independent and v as well as the quartic coupling λ are fitted to the IR masses $m_\pi = 138$ MeV and $m_\sigma = 600$ MeV, while $\langle\sigma\rangle = f_\pi = 93$ MeV is approached.

6 Application of the PTRG to the QM Model

As we will not be able to find a flow equation for our full effective average action, it is first expanded in an operator expansion [1]:

$$\Gamma_k = \int \mathrm{d}^d x \left[\Omega_k(\phi) + \frac{1}{2}(\partial_\mu\phi)^2 + \mathcal{O}(\partial^2)\right]. \tag{46}$$

We will only focus on the lowest order term, the effective potential Ω_k. Furthermore, we will treat fermions and bosons separately by splitting the Lagrangian. This includes another approximation, since the meson field ϕ will be treated as a mean background field $\langle\phi\rangle = (\langle\sigma\rangle, 0)$ in the fermionic interaction.

6.1 Fermionic Part

The fermionic Lagrangian reads

$$\mathscr{L}_\mathrm{F} = \overline{q}\,(\mathrm{i}\partial\!\!\!/ - g\,\langle\sigma\rangle)\,q. \tag{47}$$

Including a chemical quark potential, the partition function becomes

$$Z_\mathrm{F} = \int \mathcal{D}\overline{q}\mathcal{D}q \exp\left\{-\int_0^\beta \mathrm{d}\tau \int \mathrm{d}^3x\,(-\mathrm{i}\,\mathscr{L}_\mathrm{F} + \mu\,\gamma_0\,\overline{q}q)\right\}. \tag{48}$$

Here, a Wick rotation $t \to -\mathrm{i}\tau$ has been used. With the definitions

$$D\!\!\!/ := \gamma_\mu\,(\partial^\mu + \mu\,\delta_0^\mu), \qquad m_q := g\,\langle\sigma\rangle, \qquad S_0^{-1} := D\!\!\!/ + \mathrm{i}\,m_q, \tag{49}$$

the partition function takes the Gaussian form

$$Z_\mathrm{F} = \int \mathcal{D}\overline{q}\mathcal{D}q\,\exp\left\{-\left[\overline{q}\,S_0^{-1}\,q\right]\right\} = \det S_0^{-1}. \tag{50}$$

Now it is simple to express the effective action in terms of S_0^{-1}:

$$\Gamma_{\mathrm{F}} = -W_{\mathrm{F}} = -\ln Z_{\mathrm{F}} = -\ln\det S_0^{-1} = -\mathrm{Tr}\ln S_0^{-1}. \tag{51}$$

Since the effective action is approximately the (trivial) space-time integral of the effective potential (46), the latter can be written as

$$\Omega_{\mathrm{F}} = -\frac{1}{\beta V_3}\mathrm{Tr}\ln S_0^{-1}. \tag{52}$$

Again, we are at a point where the logarithm has to be regularized. Unfortunately, the Schwinger proper time formalism can not be used on the potential as it is now, because S_0^{-1} is not an elliptic operator.[1] Therefore, the operator

$$\widetilde{S_0^{-1}} := P S_0^{-1} P \quad \text{with} \quad P := \mathrm{i}\gamma_5 \tag{53}$$

is introduced. Since $\det P = -1$ and $\det(AB) = \det(A)\det(B)$, the determinants of S_0^{-1} and $\widetilde{S_0^{-1}}$ are equal. The product of the two operators is an elliptic operator

$$S_0^{-1}\widetilde{S_0^{-1}} = (\not{D} + \mathrm{i}m_q)(\not{D} - \mathrm{i}m_q) = \not{D}\not{D} + m_q^2, \tag{54}$$

where the relations

$$\gamma_5^2 = 1, \quad \gamma_\mu\gamma_5 = -\gamma_5\gamma_\mu \tag{55}$$

came to use. This enables us to re-express the partition function in terms of an elliptic operator:

$$Z_{\mathrm{F}} = \det S_0^{-1} = \det\left(S_0^{-1}\widetilde{S_0^{-1}}\right)^{\frac{1}{2}}. \tag{56}$$

Hence, the potential becomes

$$\Omega_{\mathrm{F}} = -\frac{1}{\beta V_3}\ln\left(\det\left(S_0^{-1}\widetilde{S_0^{-1}}\right)^{\frac{1}{2}}\right) = -\frac{1}{2\beta V_3}\mathrm{Tr}\ln\left(S_0^{-1}\widetilde{S_0^{-1}}\right). \tag{57}$$

In this form, it allows a regularization:

$$\Omega_{\mathrm{F,reg.}} = \frac{1}{2\beta V_3}\int_0^\infty \frac{\mathrm{d}s}{s}\, f_k(s,\Lambda^2)\,\mathrm{Tr}\,\mathrm{e}^{-s\,S_0^{-1}\widetilde{S_0^{-1}}}. \tag{58}$$

In order to evaluate the integral, the trace must first be calculated. To do this, we express the color and flavor matrix elements of $S_0^{-1}\widetilde{S_0^{-1}}$ in momentum space. Following the Dirac algebra and applying the coordinate space representation $p_\mu = \mathrm{i}\,\partial_\mu$, one receives

$$\begin{aligned}\left(S_0^{-1}\widetilde{S_0^{-1}}\right)^{ab}_{ud} &= -(p_0^2 - \vec{p}^2)\,\mathbb{1}_\gamma\,\delta_{ud} + m_q^2\,\mathbb{1}_\gamma\,\delta^{ab}\,\delta_{ud} \\ &= -p^2\,\mathbb{1}_\gamma\,\delta_{ud} + m_q^2\,\mathbb{1}_\gamma\,\delta^{ab}\,\delta_{ud},\end{aligned} \tag{59}$$

[1] A differential operator

$$P = \sum_{|\alpha|\le r} a_\alpha \partial^\alpha$$

of order r with the property

$$p(x,\xi) := \sum_{|\alpha|=r} a_\alpha \xi^\alpha \neq 0 \quad \forall\,\xi\,\epsilon\,\mathbb{R}^n \setminus 0$$

is defined as elliptic [9].

where $p_0 = \omega_n + \mathrm{i}\,\mu$. We will perform the following trace in Euclidean 4-dimensional space with imaginary time and apply the Matsubara formalism, which yields a sum over periodic frequencies ($\omega_n = (2n+1)\pi T$ for fermions) instead of an integral, since we want to study the system at finite temperatures. The trace over the Dirac space is 4 and the color and flavor spaces also trivially add their respective dimensions N_c and N_f to the product. With the change in metric of the momentum trace, the resulting flow equation is

$$\partial_t \Omega_\mathrm{F} = 2N_\mathrm{c}N_\mathrm{f}T \int_0^\infty \frac{\mathrm{d}s}{s} \left(\partial_t f_k(s,\Lambda^2)\right) \sum_n \int \frac{\mathrm{d}^3 p}{(2\pi)^3}\, \mathrm{e}^{-s\,(p_0^2+\vec{p}^2+m_q^2)}. \tag{60}$$

The momentum integration consists of three Gaussian integrals which can be computed easily:

$$\partial_t \Omega_\mathrm{F} = \frac{2N_\mathrm{c}N_\mathrm{f}T}{8\sqrt{\pi}^3} \int_0^\infty \frac{\mathrm{d}s}{s^{5/2}} \left(\partial_t f_k(s,\Lambda^2)\right) \sum_n \mathrm{e}^{-s\,(p_0^2+m_q^2)}. \tag{61}$$

Because of the scale derivation, it is sufficient to consider the k-dependent part of the regulator function. It is usually given by functions of the form

$$f(sk^2)^{(i,d)} = \frac{2^i (d-2)!!}{\Gamma(d/2)(d-2+2i)!!} \Gamma(d/2+i, sk^2), \tag{62}$$

whereas $f^{(1,3)}$ yields analytically solvable Matsubara sums. Its scale derivative,

$$\partial_t f(sk^2)^{(1,3)} = -\frac{8}{3\sqrt{\pi}} \left(sk^2\right)^{5/2} \mathrm{e}^{-sk^2}, \tag{63}$$

is used in the derivation of the PTRG flow equation for the QM model [10]. Now, the flow equation reads

$$\begin{aligned} \partial_t \Omega_\mathrm{F} &= -\frac{2N_\mathrm{c}N_\mathrm{f}k^5}{3\pi^2}\, T \sum_n \int_0^\infty \mathrm{d}s\, \mathrm{e}^{-s\,((\omega_n+\mathrm{i}\mu)^2+E_q^2)} \\ &= -\frac{2N_\mathrm{c}N_\mathrm{f}k^5}{3\pi^2}\, T \sum_n \frac{1}{(\omega_n+\mathrm{i}\,\mu)^2+E_q^2} \end{aligned} \tag{64}$$

with the squared quark energy $E_q^2 = m_q^2 + k^2$. The sum over the Matsubara frequencies can be evaluated with the help of the residue theorem. One just expresses the sum in eq. (64) by a contour integral of the summand multiplied with a function that has simple poles with residue 1 at $z = \mathrm{i}\,\omega_n$ [11]:

$$\frac{1}{\beta} \sum_n \frac{1}{(\omega_n+\mathrm{i}\,\mu)^2+E_q^2} = \frac{1}{\beta 2\pi \mathrm{i}} \int_C \mathrm{d}z\, \frac{1}{(-\mathrm{i}\,z+\mathrm{i}\,\mu)^2+E_q^2}\, u_\beta(z) \tag{65}$$

The contour goes around the imaginary axis and thus around all the poles of $u_\beta(z)$. It can be deformed into one closed contour along the imaginary axis with a small offset ε to the right (positive real part) and back in a half circle of radius $R \to \infty$ and a similar contour on the left side of the imaginary axis (negative real part), each going in clockwise direction (cf. [11]). This only holds if the absolute value of the argument of the above integral vanishes sufficiently fast for $R \to \infty$, rendering the parts along the half circles zero. A suitable weight function for fermions is

$$u_\beta(z) = \frac{\beta}{2}(1-2\,n_\mathrm{F}(z)) = \frac{\beta}{2} \tanh\left(\frac{\beta z}{2}\right), \tag{66}$$

where $n_{\mathrm{F}}(z) = (\exp(\beta z) + 1)^{-1}$ denotes the Fermi-Dirac distribution. Now, the poles on the imaginary axis are not taken into account anymore, but the poles of the original summand are within the contour. In this case, we get

$$\frac{1}{(-\mathrm{i}\, z + \mathrm{i}\, \mu)^2 + E_q^2} = \frac{1}{(E_q + (z-\mu))} \frac{1}{(E_q - (z-\mu))}, \quad z_{1,2} = \mu \pm E_q. \tag{67}$$

We see that the integral can be replaced by a sum again, but over different indices and with a modified argument:

$$\begin{aligned} \frac{1}{\beta 2\pi \mathrm{i}} \int_C \mathrm{d}z \, \frac{1}{(-\mathrm{i}\, z + \mathrm{i}\, \mu)^2 + E_q^2} \, u_\beta(z) &= -\frac{1}{2} \sum_{i=1}^{2} \operatorname*{Res}_{z=z_i} \left(\frac{1}{E_q^2 - (z-\mu)^2} \, \tanh\left(\frac{\beta z}{2}\right)\right) \\ &= \frac{1}{4E_q} \left(\tanh\left(\frac{E_q - \mu}{2T}\right) + \tanh\left(\frac{E_q + \mu}{2T}\right)\right) \end{aligned} \tag{68}$$

This is finally inserted into eq. (64) to deliver the fermionic part of the flow equation:

$$\partial_t \Omega_{\mathrm{F}} = -\frac{N_{\mathrm{c}} N_{\mathrm{f}} k^5}{6\pi^2 E_q} \left(\tanh\left(\frac{E_q - \mu}{2T}\right) + \tanh\left(\frac{E_q + \mu}{2T}\right)\right). \tag{69}$$

6.2 Bosonic Part

The derivation of the bosonic part of the flow equation follows the same strategy as the derivation of the fermionic part. Firstly, the bosonic Lagrangian in Euclidean metric is

$$\mathscr{L}_{\mathrm{B}} = \frac{1}{2} (\partial_\mu \sigma)^2 + \frac{1}{2} (\partial_\mu \vec{\pi})^2 + U(\sigma, \vec{\pi}) = \frac{1}{2} (\partial_\mu \phi)^2 + U(\phi) \tag{70}$$

with $U(\sigma, \vec{\pi}) = U(\phi)$ from equation (45) and $\phi = (\sigma, \vec{\pi})$. In this case, we can immediately calculate the second functional derivative of the effective average action Γ_{B}, which is needed in the PTRG flow equation (43). Therefore, we will express Γ_{B} in momentum space:

$$\Gamma_{\mathrm{B}}[\phi] = \int \frac{\mathrm{d}^4 p}{(2\pi)^4} \left(-\frac{1}{2} p^2 \phi(p)\phi(p) + U(\phi^2(p))\right) \tag{71}$$

As we have already done above, we will from now on write $U = U(\phi^2)$ to introduce the short-hand notation $U' = \mathrm{d}U/\mathrm{d}\phi^2$, $U'' = \mathrm{d}^2 U/(\mathrm{d}\phi^2)^2$ etc. We get

$$\frac{\delta^2 \Gamma_{\mathrm{B}}}{\delta\phi_a(p)\delta\phi_b(p')} = \left(-p^2 \delta_{ab} + 2U'\delta_{ab} + 4U''\phi_a(p)\phi_b(p')\right) \, \delta(p - p'). \tag{72}$$

This operator is elliptic and it can directly be inserted into the flow equation. Again, we need to calculate some traces:

$$\begin{aligned} \mathrm{Tr} \exp\left(-s\, \Gamma_{\mathrm{B}}^{(2)}[\phi]\right) = \beta V_3 T \sum_n \int \frac{\mathrm{d}^3 p}{(2\pi)^3} \exp\left(-s\, p^2\right) \cdot \\ \cdot \left[\exp\left(-s\, \left(2U' + 4U''\sigma^2\right)\right) + 3 \exp\left(-s\, 2U'\right)\right], \end{aligned} \tag{73}$$

where a mean field approximation $\phi = (\sigma, 0)$ has been applied to perform the trace over the meson spaces:

$$\begin{aligned} \mathrm{Tr}_{\mathrm{mes.}} \exp\left[-s\, \left(2U'\delta_{ab} + 4U''\phi_a(p) \;\; \phi_b(p)\right)\right] &\approx \mathrm{Tr}_{\mathrm{mes.}} \exp\left[-s\, \left(2U'\delta_{ab} + 4U''\sigma^2\, \delta_{ab}\right)\right] \\ &= \exp\left(-s\, \left(2U' + 4U''\sigma^2\right)\right) + 3 \exp\left(-s\, 2U'\right). \end{aligned} \tag{74}$$

The three Gaussian momentum integrals and the proper time integral are left to be evaluated and under the usage of the same regulator function $f(sk^2)^{(1,3)}$ as in the fermion part, all this leads to

$$\partial_t \Omega_{\mathrm{B}} = -\frac{k^5}{6\pi^2} T \sum_n \left(\frac{1}{k^2 + \omega_n^2 + 2U' + 4U''\sigma^2} + \frac{3}{k^2 + \omega_n^2 + 2U'} \right). \tag{75}$$

The Matsubara frequencies $\omega_n = -\mathrm{i}\, p_0 = 2n\pi T$ are even for Bosons. Thus, the weight function changes to

$$u_\beta(z) = \frac{\beta}{2}(1 + 2\, n_{\mathrm{B}}(z)) = \frac{\beta}{2} \coth\left(\frac{\beta z}{2}\right). \tag{76}$$

in order to produce poles at the correct frequencies. $n_{\mathrm{B}}(z) = (\exp(\beta z) - 1)^{-1}$ is the Bose-Einstein statistics. A chemical potential is not included and the residues at the relevant poles are summed up in

$$\sum_{i=1}^{2} \operatorname*{Res}_{z=z_i} \left(\frac{1}{E_j^2 - z^2} \coth\left(\frac{\beta z}{2}\right) \right) = -\frac{1}{E_j} \coth\left(\frac{E_j}{2T}\right), \tag{77}$$

where $z_i = \pm E_j$ for $E_1^2 = k^2 + 2U' + 4U''\sigma^2$ and $E_2^2 = k^2 + 2U'$ respectively. This result has to be multiplied with $\beta/2$ from the weight function and inserted into the bosonic flow equation (75) for the complete results for the bosonic part:

$$\partial_t \Omega_{\mathrm{B}} = \frac{k^5}{12\pi^2} \left(\frac{1}{E_\sigma} \coth\left(\frac{E_\sigma}{2T}\right) + \frac{3}{E_\pi} \coth\left(\frac{E_\pi}{2T}\right) \right). \tag{78}$$

Here, the energies have already been indexed with the corresponding meson field. On top of that, the renormalization group improvement has been used one more time by replacing the mesonic potential $U(\phi^2)$ with the full effective potential $\Omega_k(\phi^2)$, which is not truncated at the order 2. Bringing the pieces together, the full PTRG flow equation in application to the quark-meson model becomes [7]

$$\begin{aligned} \partial_t \Omega_k(\phi^2) = \frac{k^5}{12\pi^2} \Bigg\{ & \frac{1}{E_\sigma} \coth\left(\frac{E_\sigma}{2T}\right) + \frac{3}{E_\pi} \coth\left(\frac{E_\pi}{2T}\right) \\ & - \frac{2N_{\mathrm{c}} N_{\mathrm{f}}}{E_q} \left[\tanh\left(\frac{E_q + \mu}{2T}\right) + \tanh\left(\frac{E_q - \mu}{2T}\right) \right] \Bigg\}. \end{aligned} \tag{79}$$

The energies are

$$\begin{aligned} E_\pi &= \sqrt{k^2 + m_\pi^2} = \sqrt{k^2 + 2\Omega_k'}, \\ E_\sigma &= \sqrt{k^2 + m_\sigma^2} = \sqrt{k^2 + 2\Omega_k' + 4\phi^2 \Omega_k''}, \\ E_q &= \sqrt{k^2 + m_q^2} = \sqrt{k^2 + g^2\phi^2}. \end{aligned} \tag{80}$$

7 Evaluation of the PTRG Flow Equation

The PTRG flow equation we found for the quark-meson model (79) is a (functional) partial differential equation and it is not analytically solvable as far as we know by now. It can be tackled by either a discretization of the potential on a grid or a Taylor series expansion [10]. In this work, the latter is done. We expand the potential in terms of ϕ^2 around a global minimum ϕ_0^2. Since we only examine the radial component of the field and do not know the single components (which also do not differ in their contributions in the chiral limit), we will from now on substitute the variable ϕ^2 by σ^2, which shall also be the direction to be distinguished by the explicit symmetry breaking term.

7.1 Chiral Symmetry

First, we will explore the system under chiral symmetry. This means that no explicit symmetry breaking term is used, i.e. $c = 0$ in the meson potential (45). In a Taylor series expansion, the effective potential then reads

$$\Omega_k(\sigma^2) = \sum_{j=0}^{N} \frac{1}{j!}\, a_j\, (\sigma^2 - \sigma_0^2)^j \tag{81}$$

The sum is truncated at the order N, which means that, including the 0th term, we will get a system of $N+1$ coupled ordinary differential equations for the k-dependent expansion coefficients

$$a_j = a_{j,k} = \Omega_k^{(j)}(\sigma^2)\Big|_{\sigma=\sigma_0} = \Omega_k^{(j)}(\sigma_0^2), \tag{82}$$

where the uppercase index in parenthesis denotes the jth derivative with respect to σ^2. At the beginning of the evaluation, the minimum of the potential shall be at $\sigma_0 \equiv 0$. In other words, at the UV cutoff, the fields should be zero. The Taylor expansion simplifies to

$$\Omega_k(\sigma^2) = \sum_{j=0}^{N} \frac{1}{j!}\, a_j\, (\sigma^2)^j. \tag{83}$$

A Taylor expansion of the flow equation $\partial_t \Omega_k$ yields

$$\partial_t \Omega_k(\sigma^2) = \sum_{j=0}^{N} \frac{1}{j!}\, (\partial_t \Omega_k)^{(j)}(0)\, (\sigma^2)^j, \tag{84}$$

while a partial differentiation of $\Omega_k(\sigma^2)$ (83) with respect to t results in

$$\partial_t \Omega_k(\sigma^2) = \sum_{j=0}^{N} \frac{1}{j!} \left(\frac{\mathrm{d}}{\mathrm{d}t} a_j\right) (\sigma^2)^j, \tag{85}$$

which immediately implies

$$\frac{\mathrm{d}}{\mathrm{d}t} a_j = \partial_t \Omega_k^{(j)}(\sigma^2)\Big|_{\sigma=0}. \tag{86}$$

The right-hand side of the equation is found by taking the jth derivative of the PTRG flow equation (79) with respect to σ^2 and evaluating the result at $\sigma = 0$. This is done

in appendix A. One can see that under these conditions, the flow equation degenerates in the way that the pion and sigma energies (80) at the minimum of the potential are equal:

$$E_\pi|_{\sigma=0} = E_\sigma|_{\sigma=0} = \sqrt{k^2 + 2\Omega_k'|_{\sigma=0}} = \sqrt{k^2 + 2a_1} =: E_m. \tag{87}$$

The bosonic parts of the flow equation are now summed up in one term. Furthermore, the quarks are massless. The flow equation then reads

$$\partial_t \Omega_k(\sigma^2 = 0) = \frac{k^5}{12\pi^2} \left\{ \frac{4}{E_m} \coth\left(\frac{E_m}{2T}\right) - \frac{2N_\mathrm{c}N_\mathrm{f}}{k} \left[\tanh\left(\frac{k+\mu}{2T}\right) + \tanh\left(\frac{k-\mu}{2T}\right)\right]\right\}. \tag{88}$$

7.2 Spontaneous Symmetry Breaking

The fermionic part in (88) gets stronger with decreasing k, which will eventually cause the expansion coefficient a_1 to drop to negative values. This is not a physical behaviour, e.g. the square of the meson masses (87) becomes negative. The solution to this problem is to go back to the original Taylor expansion (81) and allow a finite global minimum σ_0^2 of the potential in the evolution from the point a_1 becomes 0 onward. We just demand

$$a_1 \equiv \Omega_k'(\sigma_0^2) \stackrel{!}{=} 0, \tag{89}$$

which is the necessary criterion for a local minimum at σ_0^2. We lose one differential equation and, of course, it has to be replaced by another one for the system to be described in its entirety. This makes perfect sense, as the minimum $\sigma_0^2 = \sigma_{0,k}^2$ is now scale dependent and shifts during the evolution of the flow equation towards the IR. We remember that this *spontaneous symmetry breaking* happens at the *chiral symmetry breaking scale* k_χ. A differential equation for σ_0^2 remains to be found and the other differential equations have to be adjusted to include a scale-dependent minimum. To do this, we will again partially differentiate the Taylor expansion of the potential (81):

$$\begin{aligned}
\partial_t \Omega_k(\sigma^2) &= \sum_{j=0}^{N} \frac{1}{j!} \left(\frac{\mathrm{d}}{\mathrm{d}t} a_j\right) (\sigma^2 - \sigma_0^2)^j + \sum_{j=1}^{N} \frac{1}{(j-1)!} a_j (\sigma^2 - \sigma_0^2)^{j-1} \left(-\frac{\mathrm{d}}{\mathrm{d}t}\sigma_0^2\right) \\
&= \sum_{j=0}^{N} \frac{1}{j!} \left[\left(\frac{\mathrm{d}}{\mathrm{d}t} a_j\right) - a_{j+1}\left(\frac{\mathrm{d}}{\mathrm{d}t}\sigma_0^2\right)\right] (\sigma^2 - \sigma_0^2)^j \\
&= \sum_{j=0}^{N} \frac{1}{j!} \left[\left(\frac{\mathrm{d}}{\mathrm{d}t} \Omega_k^{(j)}(\sigma_0^2)\right) - \Omega_k^{(j+1)}(\sigma_0^2)\left(\frac{\mathrm{d}}{\mathrm{d}t}\sigma_0^2\right)\right] (\sigma^2 - \sigma_0^2)^j \\
&= \sum_{j=0}^{N} \frac{1}{j!} \left(\partial_t \Omega_k^{(j)}(\sigma_0^2)\right) (\sigma^2 - \sigma_0^2)^j.
\end{aligned} \tag{90}$$

We also would have gotten the last result, if we had just expanded $\partial_t \Omega_k(\sigma^2)$ in a Taylor series around σ_0^2. It is important to keep in mind the difference between a partial differentiation $\partial_t = \frac{\partial}{\partial t}$, where the scale dependence of the actual variable in parenthesis is neglected, and a total differentiation $\frac{\mathrm{d}}{\mathrm{d}t}$, where it is included. Comparing the second and the last row of the above equation, we find the modified differential equation for the expansion coefficients:

$$\frac{\mathrm{d}}{\mathrm{d}t} a_j = \partial_t \Omega_k^{(j)}(\sigma^2)\Big|_{\sigma=\sigma_0} + a_{j+1} \frac{\mathrm{d}}{\mathrm{d}t}\sigma_0^2. \tag{91}$$

The interpretation of the last term is that it includes the running of the minimum, hence of the expansion point. This is now a tower of N coupled differential equations, where the last term does not include the running of σ_0^2, because $a_{N+1} = \Omega_k^{(N+1)}(\sigma_0^2) = 0$. Since we imposed $\frac{\mathrm{d}}{\mathrm{d}t} a_1 \equiv 0$ (which means that σ_0^2 stays a local minimum throughout the evaluation), equation (91) also gives us the differential equation for σ_0^2:

$$\frac{\mathrm{d}}{\mathrm{d}t}\sigma_0^2 = -\frac{1}{a_2}\,\partial_t \Omega_k'(\sigma^2)\big|_{\sigma=\sigma_0}\,. \tag{92}$$

Due to the vanishing derivative of the effective potential at the minimum, the pion masses vanish there as well:

$$\begin{aligned} m_{\pi,\sigma_0}^2 &= 2\Omega_k'(\sigma_0^2) = 0 \\ m_{\sigma,\sigma_0}^2 &= 2\Omega_k'(\sigma_0^2) + 4\sigma_0^2\Omega_k''(\sigma_0^2) = 4\,\sigma_0^2\,a_2 \\ m_{q,\sigma_0}^2 &= g^2\sigma_0^2. \end{aligned} \tag{93}$$

7.3 Explicit Symmetry Breaking

In order to produce finite pion masses, an explicit symmetry breaking term is introduced. The potential now reads

$$\widetilde{\Omega}_k(\sigma^2) = \sum_{j=0}^{N} \frac{1}{j!}\, b_j\,(\sigma^2 - \sigma_0^2)^j - c\sigma, \tag{94}$$

where c is a positive k-independent scalar. As the sum is still a Taylor series expansion, it has to be the expansion of $\Omega_k = \widetilde{\Omega}_k + c\sigma$. Therefore, the coefficients still read

$$b_j = \Omega_k^{(j)}(\sigma_0^2). \tag{95}$$

On top of that, the scale independence of c has the advantage that $\partial_t\widetilde{\Omega}_k(\sigma^2) = \partial_t\Omega_k(\sigma^2)$, where $\partial_t\Omega_k(\sigma^2)$ is known from the flow equation. Inserting $\widetilde{\Omega}_k$ into the differential equation would lead to different results, since the explicit symmetry breaking term does not disappear being differentiated with respect to σ^2. This conflict can only be solved under the premise that the flow equation is incorrect for unsymmetric potentials. This can be understood, since only the squared fields and derivations with respect to these are used in the derivation, which means that only the radial component is considered. Fortunately, as already stated, a partial differentiation with respect to t shows that both potentials obey the same differential equation. Consequently, the Taylor expanded ordinary differential equations stay the same as the ones under spontaneous symmetry breaking (91). The main difference, however, is that the expansion point has changed. We want to know the potential $\widetilde{\Omega}_k$ near its global minimum, which is characterized by

$$\widetilde{\Omega}_k'(\sigma_0^2) = \Omega_k'(\sigma_0^2) - c\left(\frac{\mathrm{d}}{\mathrm{d}\sigma^2}\sigma\right)\bigg|_{\sigma=\sigma_0} = b_1 - \frac{c}{2\sigma_0} \overset{!}{=} 0 \quad\Longleftrightarrow\quad b_1 = \frac{c}{2\sigma_0}. \tag{96}$$

To differentiate σ with respect to σ^2, the trick

$$\frac{\mathrm{d}}{\mathrm{d}\sigma^2} = \frac{\mathrm{d}}{2\sigma\mathrm{d}\sigma} = \frac{1}{2\sigma}\frac{\mathrm{d}}{\mathrm{d}\sigma}$$

was used. It is notable that $\sigma_0 = 0$ is not allowed for b_1 to stay finite, consequently there is always a positive minimum of the potential and thus the chiral symmetry is

always broken for $c > 0$. b_1 is now scale-dependent, so the relation $\frac{\mathrm{d}}{\mathrm{d}t} b_1 = 0$ can not hold anymore and the derivation of the differential equation for σ_0^2 becomes wrong. We can correct it by using the relation

$$\begin{aligned} 0 \overset{!}{=} \frac{\mathrm{d}}{\mathrm{d}t}\left(b_1 - \frac{c}{2\sigma_0}\right) &\overset{(91)}{=} \partial_t \Omega_k'(\sigma_0^2) + b_2 \frac{\mathrm{d}}{\mathrm{d}t}\sigma_0^2 + \frac{c}{4\sigma_0^3}\frac{\mathrm{d}}{\mathrm{d}t}\sigma_0^2 \\ \iff \quad \frac{\mathrm{d}}{\mathrm{d}t}\sigma_0^2 &= -\frac{1}{b_2 + \frac{c}{4\sigma_0^3}}\ \partial_t \Omega_k'(\sigma^2)\big|_{\sigma=\sigma_0}\,. \end{aligned} \tag{97}$$

Remarkably, the particle energies are still found by taking Ω_k instead of $\widetilde{\Omega}_k$ in the energy equations (80), because c does not change in the evolution process and, as already stated, the original Taylor expansion without explicit symmetry breaking term has to be used in the flow equation. Plugging in the known value for b_1, we get a finite pion mass:

$$\begin{aligned} m_{\pi,\sigma_0}^2 &= \frac{c}{\sigma_0} \\ m_{\sigma,\sigma_0}^2 &= \frac{c}{\sigma_0} + 4\,\sigma_0^2\, b_2 \\ m_{q,\sigma_0}^2 &= g^2\sigma_0^2. \end{aligned} \tag{98}$$

In the numerical evolution, we are now able to set the starting values accordingly to receive correct final IR values. First of all, we will fit σ_0 to the pion decay constant $\sigma_{0,\mathrm{IR}} = f_\pi = 93$ MeV. To get an effective quark mass of about 300 MeV, $g = m_{q,\mathrm{IR}}/\sigma_{0,\mathrm{IR}} = 3.22$ follows, while a pion mass of 138 MeV implies $c = m_{pi,\mathrm{IR}}^2 \cdot \sigma_{0,\mathrm{IR}} = 1,771,092$ MeV^3. $b_{2,\mathrm{IR}} = 9.86$ follows from a sigma mass of 600 MeV.

7.4 The QM Model Revisited

In this short section, the expansion coefficients of the effective potential shall be related to the parameters λ and v of the mesonic potential quark-meson model. As we have seen above, the coefficients for the linear and the quadratic term are deciding for the IR masses of the particles. If we just add and substract the minimum σ_0^2 in the mesonic potential and substitute ϕ^2 by σ^2, we can factor out equation (45) and relate λ and v to σ_0 and b_2:

$$\begin{aligned} U(\sigma^2) &= \frac{\lambda}{4}(\sigma^2 - \sigma_0^2 + \sigma_0^2 - v^2)^2 - c\sigma \\ &= \frac{\lambda}{4}(\sigma^2 - \sigma_0^2)^2 + \frac{\lambda}{2}(\sigma_0^2 - v^2)(\sigma^2 - \sigma_0^2) + \frac{\lambda}{4}(\sigma_0^2 - v^2)^2 - c\sigma. \end{aligned} \tag{99}$$

By comparison of the first term of the mesonic potential and the quadratic term in $\widetilde{\Omega}_k$, we immediately find $\lambda = 2\,b_2$. Using $b_1 = c/(2\sigma_0)$, the linear term yields $v^2 = \sigma_0^2 - c/(\sigma_0\lambda)$.

7.5 Contributions to the Flow

It will turn out to be helpful to understand if and when the respective meson or quark fields produce the main contributions to the flow. Therefore, we regard the limit $T = 0$, $\mu = 0$. The flow equation then reads

$$\partial_t \Omega_k = \frac{k^5}{12\pi^2}\left(\frac{1}{E_\sigma} + \frac{3}{E_\pi} - \frac{4N_\mathrm{c}N_\mathrm{f}}{E_q}\right), \tag{100}$$

since the *threshold functions* yield 1 (for positive arguments):

$$\begin{aligned} \coth\left(\frac{E}{2T}\right) &\xrightarrow{T\to 0} 1, \quad E > 0, \\ \tanh\left(\frac{E\pm\mu}{2T}\right) &\xrightarrow{T\to 0} 1, \quad E\pm\mu > 0. \end{aligned} \tag{101}$$

In the chiral limit, the quark mass at the minimum is zero, thus the quark energy is the lowest energy term in the equation. With the additional degrees of freedom from the color and flavor numbers, the main contribution to the flow comes from the quarks. Since the evolution happens downwards ($\mathrm{d}k < 0$), the sign of the flow equation has to be changed in order to get an indication about the direction of the flow evolution. Consequently, $a_0 = \Omega_k(0)$ will increase to positive values and $a_1 = \Omega_k'(0)$ will decrease, because the derivation of $1/E_q$ with respect to σ^2 changes the sign. That means that the quarks drive the evolution towards the spontaneous symmetry breaking, while the mesons work against it. Under spontaneous symmetry breaking, the same argumentation holds. The sign of the flow of σ_0^2 is opposite to the one of a_1 from before, which can be verified in (92). Thus, the quarks increase the minimum, while the meson contributions try to restore the chiral symmetry. If one goes to non-vanishing temperatures, the threshold functions must be included. The contributions of the quarks diminish due to

$$\tanh\left(\frac{E\pm\mu}{2T}\right) \xrightarrow{(E\pm\mu)/2T\to 0} 0, \tag{102}$$

while the meson contributions increase:

$$\coth\left(\frac{E}{2T}\right) \xrightarrow{E/2T\to 0} \infty, \quad E > 0,\, T > 0. \tag{103}$$

At a critical temperature T_c, they are strong enough to restore the chiral symmetry, as we will see later.

In the spontaneously broken phase, the quark masses steadily increase and the pion masses are zero at the minimum, so $E_{\pi,\sigma_0} = k \xrightarrow{k\to 0} 0$. Hence, the flow is mainly governed by the pion fluctuations for small k. This enables us to qualitatively predict the running of the higher order coefficients a_3, a_4 etc. Due to the high exponents of the energy terms in the denominator, the flow of these coefficients is suppressed at high scales. At very small scales, it is determined by the contributions of the pion energy term with the highest exponent in the denominator. As the sign of this term changes with every derivation, these coefficients evolve towards $+\infty$ and $-\infty$ in turn.

8 Numerical Results

For numerically solving the system of ordinary differential equations, an eighth-order Dormand-Prince method, which is a Runge-Kutta algorithm, is used (cf. [12]). It has to be modified to automatically switch from the symmetric to the broken phase when a_1 drops below 0, precisely when $-e \leq a_1 \leq 0$, where e is a small definable error. The system is examined with two quark flavours and three colors. The constants used in the evaluation are listed below.

	chiral symmetry	explicit symmetry breaking
c [MeV^3]	0	1,771,092
g	3.2	3.22
N_c	3	3
N_f	2	2

Table 1: constants of the flow equation

8.1 Initial Values

In the following, the truncation orders $N = 3, 4, 5, 6$ will be used. In order to make the results comparable, it is essential that they all have equal infrared values. Consequently, their starting values will differ. To resemble the quark-meson potential at the UV cutoff Λ, all initial values but a_1 and a_2 or σ_0^2 and b_2, respectively, are set to zero. The two remaining initial values are set accordingly to match the particle masses and the pion decay constant for $k \to 0$, as shown in section 7.3. For $c = 0$, the pion mass vanishes under spontaneous symmetry breaking and the sigma mass is reduced. Actually, the sigma mass also vanishes for $k \to 0$, because $a_2 \to 0$ converges against a Gaussian fixed point [13]. Since the numerics only allow an evaluation to a certain point $k > 0$, we will stop at $k = 1$ MeV. At this point, there are still massive sigma mesons. It has turned out that a sigma mass of $m_{\sigma,0} = \sqrt{4\sigma_0^2 a_2} \approx 248\,\mathrm{MeV}$ leads to sensible results for both UV cutoffs ($\Lambda = 950\,\mathrm{MeV}$ and $\Lambda = 1500\,\mathrm{MeV}$) that are used. According to grid simulations and chiral perturbation theory, the pion decay constant in the chiral limit is $f_\pi \approx 88$ MeV [10], which will be used as the second condition, generating a quark mass of $m_q = g f_\pi = 3.2 \cdot 88\,\mathrm{MeV} = 281.6$ MeV.

Fitting the initial values to the correct infrared values needs a sophisticated method, because variations of the starting values can change the IR values quite unpredictably. This is done via a heuristic algorithm called *differential evolution* (cf. [14]). Its feature is to globally minimize a function with a low risk of getting trapped in a local minimum. The algorithm begins by randomly producing a number of NP D-dimensional vectors. D is the number of parameters that need to be fixed; in this work, $D = 2$. Each vector is assigned a cost $C(v_i)$, which shall be minimized. This is in general a function of the D input parameters. In our case, totally random initial values would not make any sense, because the flow equation would only converge in a few cases. Therefore, it is convenient to produce random numbers only in a certain area which is near the suspected minimum.

Now, the algorithm picks three different, random vectors, a, b and c, from the NP ones that are in storage. The idea is to produce a new trial vector out of them and

compare it to the first vector in storage, v_1. Therefore, the first of the D components to set is randomly chosen. If it is the last component or if a random number (e.g. between 0 and 1) is below a prefixed constant CR, this component of the trial vector is set to $t_i = c_i + F \cdot (a_i - b_i)$, where F is another prefixed constant. Otherwise, this component gets the value of v_{1i}. This means that a high value for CR causes a strong mixing of the vectors, while a small value causes a more static behaviour. The value for F determines how big the parameter change can be. If this value is high, it is likely that many new vectors outside the area of random vectors we have set at the beginning are produced. A value of 0.5 for both constants led to good results in this work.

Now, the $D-1$ remaining components of the trial vector are generated in the same way, still using v_1 and a, b, c from before. At the end, the cost of v_1 and the trial vector are compared. If the cost (which should be minimized) of the trial vector is lower, t is saved; otherwise, v_1 is saved. All this is repeated for the other $NP-1$ vectors. Then all of them are replaced by the saved ones. The whole process is repeated until a fixed number of generations is reached. Raising NP or the number of generations significantly improves the result, but it also gets as much more time consuming. If the algorithm converges in time, all of the NP vectors are equal up to a small error and the ideal initial values are found. Minimizing the added squares (that can not assume negative values) of the differences between the actual value and the target value, namely, in the chiral limit

$$S := (\sigma_0 - 88\,\mathrm{MeV})^2 + (m_q - 281.6\,\mathrm{MeV})^2 + (m_\sigma - 275\,\mathrm{MeV})^2 \tag{104}$$

and with explicit symmetry breaking

$$B := (\sigma_0 - 93\,\mathrm{MeV})^2 + (m_q - 300\,\mathrm{MeV})^2 + (m_\pi - 138\,\mathrm{MeV})^2 + (m_\sigma - 600\,\mathrm{MeV})^2, \tag{105}$$

we get the following results:

N	Λ [MeV]	$a_{1,\Lambda}$ [MeV^2]	$a_{2,\Lambda}$	$\sigma_{0,\mathrm{IR}}$ [MeV]	$m_{q,\mathrm{IR}}$ [MeV]	$m_{\sigma,\mathrm{IR}}$ [MeV]
3	950	165622.4	5.9329	88.00	281.60	248.00
4		65423.8	13.8855	88.00	281.60	248.00
5		143500.0	9.1809	88.61	283.55	245.34
6		131847.0	8.7230	88.00	281.61	248.01
3	1500	801808.0	0.7548	88.00	281.60	248.00
4		514660.5	12.1205	88.00	281.60	248.00
5		271100.0	23.2722	88.00	281.60	248.00
6		700665.7	4.6815	88.00	281.60	248.00

Table 2: Initial values and IR values for the chiral limit

N	Λ [MeV]	$\sigma^2_{0,\Lambda}$ [MeV^2]	$a_{2,\Lambda}$	$\sigma_{0,\mathrm{IR}}$ [MeV]	$m_{q,\mathrm{IR}}$ [MeV]	$m_{\pi,\mathrm{IR}}$ [MeV]	$m_{\sigma,\mathrm{IR}}$ [MeV]
3	950	28.1795	6.69238	93.15	299.93	137.89	600.00
4		124.9274	14.16164	93.15	299.93	137.89	600.00
5		1546.6320	20.87550	93.15	299.93	137.89	600.04
6		38.4479	8.89184	93.15	299.93	137.89	600.00
3	1500	1.22824	1.49027	93.15	299.93	137.89	600.00
4		2.56637	11.57016	93.15	299.94	137.89	600.02
5		4.19307	16.84657	93.15	299.93	137.89	600.03
6		1.50897	4.69766	93.15	299.93	137.89	600.12

Table 3: Initial values and IR values for explicit symmetry breaking

Only the values for $N = 5$, $\Lambda = 950$ MeV could not be fitted perfectly.

8.2 Evolution for Vanishing Temperature and Chemical Potential

To get a general view of the dynamics of the system, we will first examine it for $T = 0$ and $\mu = 0$ under chiral symmetry as well as explicit symmetry breaking.

8.2.1 Chiral Limit

Figure 1 shows the expansion coefficients a_0 to a_2 for the truncation order $N = 3$ and a UV cutoff $\Lambda = 950$ MeV. One can see that a_1 drops rapidly, as expected due to the strong contributions of the massless quarks, spontaneously breaking the chiral symmetry at $k_\chi = 683.5$ MeV. From that point, a_1 stays zero and the minimum σ_0^2 increases. It converges against a certain value, becoming almost constant for small scales where the now massive quarks have decoupled from the flow. a_0, which is the potential Ω_k, evaluated at the global minimum, steadily increases as the fluctuations are added up. It is continuously differentiable at the chiral symmetry breaking scale, because the term that has to be added to the flow to account for a non-constant minimum, $a_1 \frac{\mathrm{d}}{\mathrm{d}t}\sigma_0^2$ (cf. (91)), is zero, since $a_1 \equiv 0$. The quartic coupling however, expressed by $a_2 \sim \lambda$, is not smooth. The kink that can be observed comes solely from the addition of the previously mentioned term. The rapid decrease of a_2 towards zero for $k \to 0$ due to the massless pion contributions can be observed here.

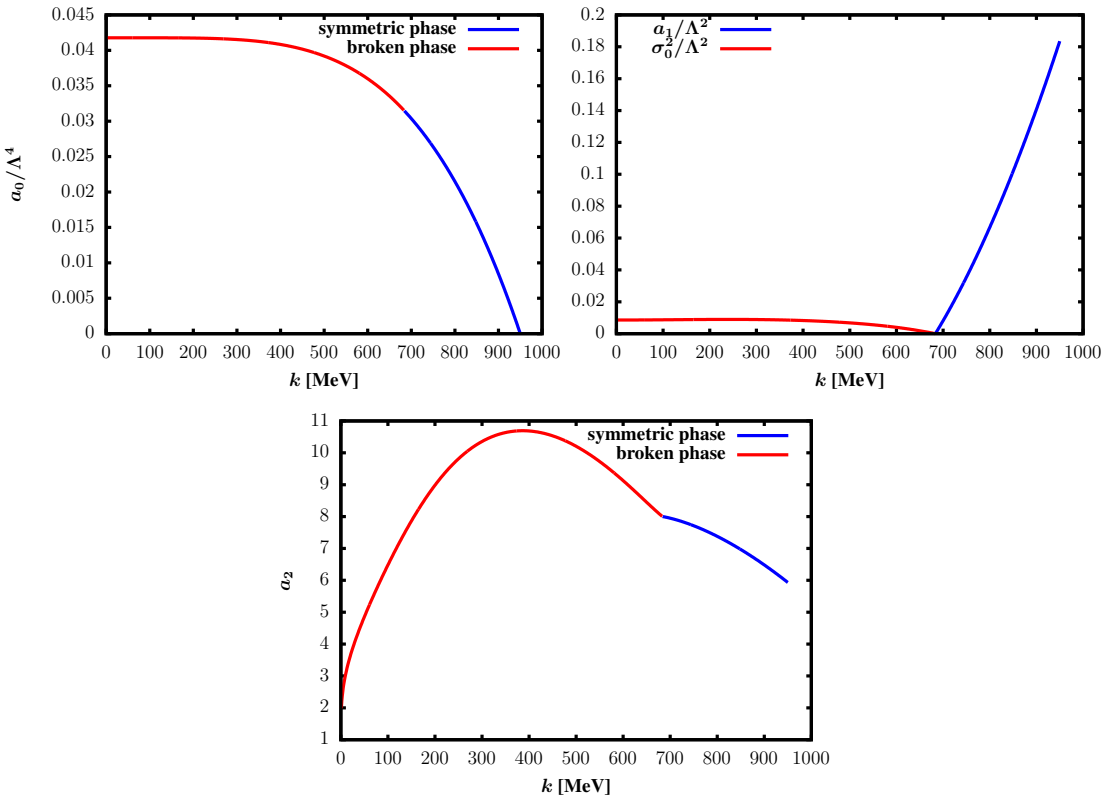

Figure 1: Expansion coefficients for order $N = 3$ and UV cutoff $\Lambda = 950$ MeV in the chiral limit. The symmetric phase is depicted in blue, the broken phase in red. a_1 is switched to σ_0^2 in the broken phase.

In figure 2, the minimum and a_2 are explored for the UV cutoff $\Lambda = 1500$ MeV and the truncation orders 3, 4, 5 and 6. As the values at $k = 0$ are set equal, the initial values differ from each other. There is no trivial connection between the truncation order and the correct set of the initial values. Although only the final IR values are of physical importance, the initial values theoretically should be obtained if the QCD with an infinite UV cutoff could be evaluated down until Λ and correctly mapped to this model. The starting values already differing this much for different truncation orders depict the problem of consistently solving QCD quite well.

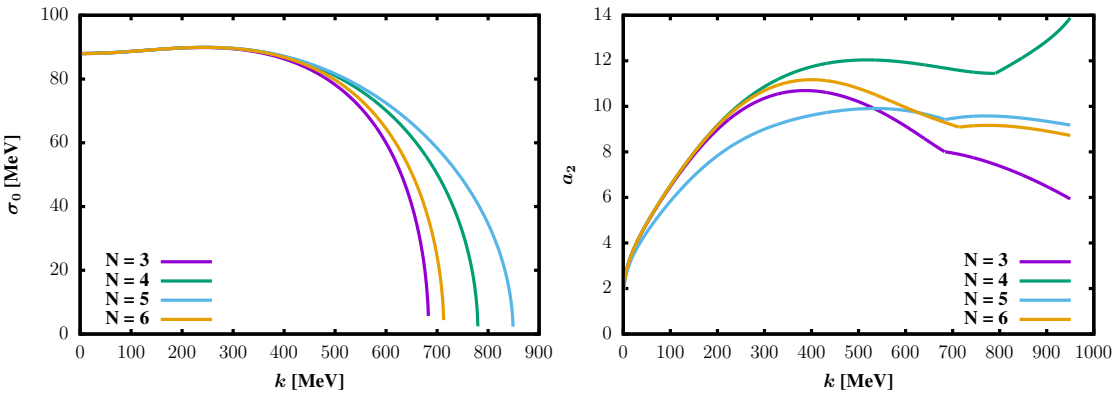

Figure 2: σ_0 and a_2 in the chiral limit for a UV cutoff $\Lambda = 1500$ MeV and the truncation orders 3–6. σ_0 only differs from 0 in the spontaneously broken phase.

8.2.2 Explicit Symmetry Breaking

Figure 3 shows σ_0 and b_2 using an explicit symmetry breaking term for $\Lambda = 1500$ MeV and the truncation orders 3–6. As the symmetry is broken right from the beginning, all the coefficients stay smooth throughout the evaluation. σ_0 typically begins at very small values and only runs weakly at high values of k, which is due to the high particle energies, where $E \sim k$ for small masses. For small values of k, the quark and meson masses, which have increased with the minimum, are high enough to weaken the running of σ_0 again. Both σ_0 and b_2 could be fitted to the correct values at all truncation orders.

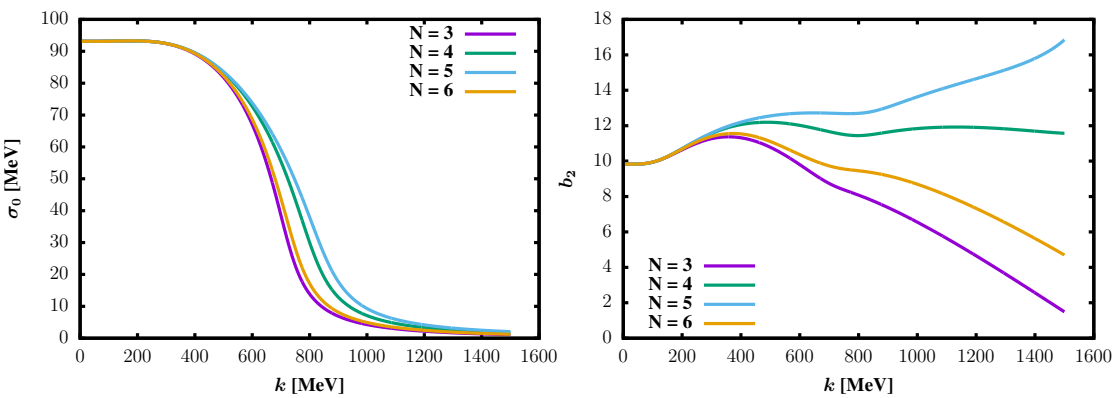

Figure 3: σ_0 and b_2 for explicit symmetry breaking, a UV cutoff $\Lambda = 1500$ MeV and the truncation orders 3–6.

8.3 Evolution for Non-Vanishing Temperature

In this section, the system will be regarded for $T > 0$. We will find a critical exponent in the chiral limit and conclude on the other critical exponents of this universality class.

8.3.1 Chiral Limit

Figure 4 shows a_1 and, as soon as it hits zero, σ_0 as well as a_2 for several temperatures for the UV cutoff $\Lambda = 1500$ MeV and $N = 6$. Due to increasing pion fluctuations in the broken phase, an increase in temperature decreases the value of $\sigma_{0,k=0}$. At the critical temperature T_c, the chiral symmetry is restored. This will hold for all higher temperatures. The curve for $T = 200$ MeV does not even hit the x-axis once, which means that spontaneous symmetry breaking does not occur on any scale for that temperature (and above). However, this result is questionable, because using the same initial values for finite temperatures as the ones we found for $T = 0$ only works if the threshold function delivers a value close to 1 at the UV cutoff [13]. As we will later see, this approach does not deliver reliable results for high temperatures. It can also be observed that a_2 gets very close to zero for increasing temperatures, which effectively renders the sigma mass zero as well.

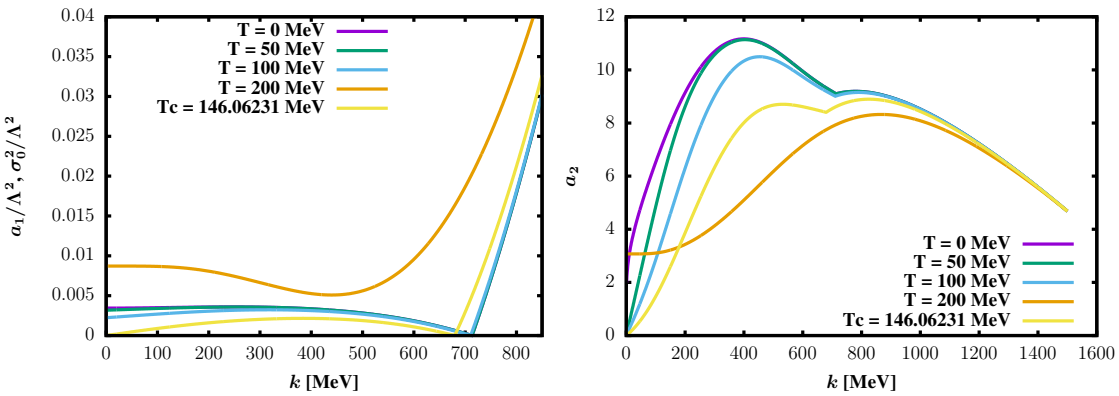

Figure 4: a_1, σ_0^2 and a_2 for a UV cutoff $\Lambda = 1500$ MeV at different temperatures. The truncation order is $N = 6$. As soon as a_1 hits zero, it is switched to σ_0^2 and vice versa.

The temperature dependency of the minimum $\sigma_{0,k=0}$ is depicted in figure 5 for several truncation orders. σ_0 is an order parameter of the system that continuously goes to zero. This means that the system experiences a second order phase transition at the critical temperature T_c where σ_0 becomes zero. For $T < T_c$, the approach can be described by the non-linear relation [13]

$$\sigma_0 \sim \left| \frac{T - T_c}{T_c} \right|^{\beta}, \tag{106}$$

where β is a critical exponent.

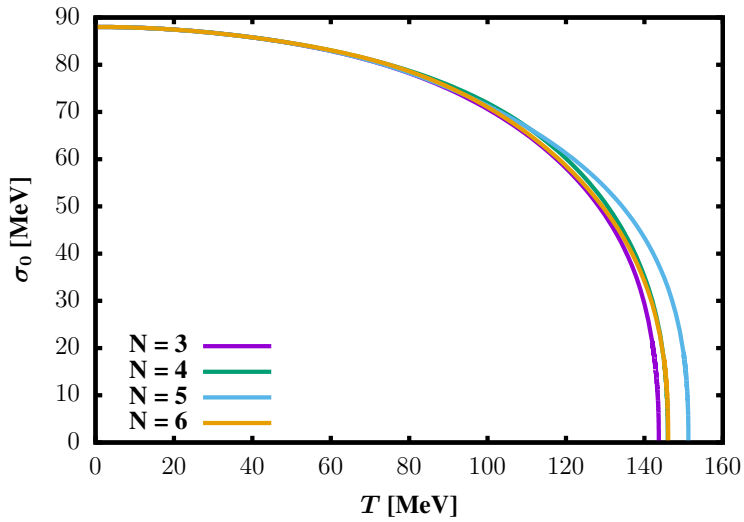

Figure 5: $\sigma_{0,k=0}$ for all temperatures up to the critical temperature T_c and the truncation orders 3–6. The UV cutoff is $\Lambda = 1500$ MeV.

Taking the logarithm on both sides, one obtains

$$\ln\left(\frac{\sigma_0}{\Lambda}\right) = \beta \ln\left(\frac{T - T_c}{T_c}\right) + C, \tag{107}$$

which is an easy to handle linear relation. In the left diagram of figure 6, a line has been fitted to the numerical results for $N = 6$ and $\Lambda = 1500$ MeV. For x-values between 0 and -4, the data points are too far away from the critical temperature and are therefore neglected. One can see that they deviate from a straight line near 0. The values between -18 and -8 on the x-axis also have to be neglected, since they get too small and a correct computation can not be assured. Fitting the line to the remaining values, one gets the critical exponents shown in the right diagram. For a truncation order of 3, β is near 0.42; for all higher orders, it is very close to 0.4. Furthermore, an oscillation around 0.4 can be observed.

$\beta = 0.4$ is the exact value for this model in the three-dimensional $O(4)$ universality class. It is three-dimensional, because the singularity $T/k \to \infty$ for finite temperatures forces a dimensional reduction. Using the scaling relations

$$\begin{aligned} \alpha &= 2 - d\nu \\ \beta &= \frac{\nu}{2}(d - 2 + \eta) \\ \gamma &= (2 - \eta)\nu \\ \delta &= \frac{d + 2 - \eta}{d - 2 + \eta}, \end{aligned} \tag{108}$$

where $d = 3$ is the dimension and $\eta = 0$ is known, because no wave function renormalization is used [13], we find the other critical exponents:

$$\begin{aligned} \nu &= 0.8 \\ \alpha &= -0.4 \\ \gamma &= 1.6 \\ \delta &= 5. \end{aligned} \tag{109}$$

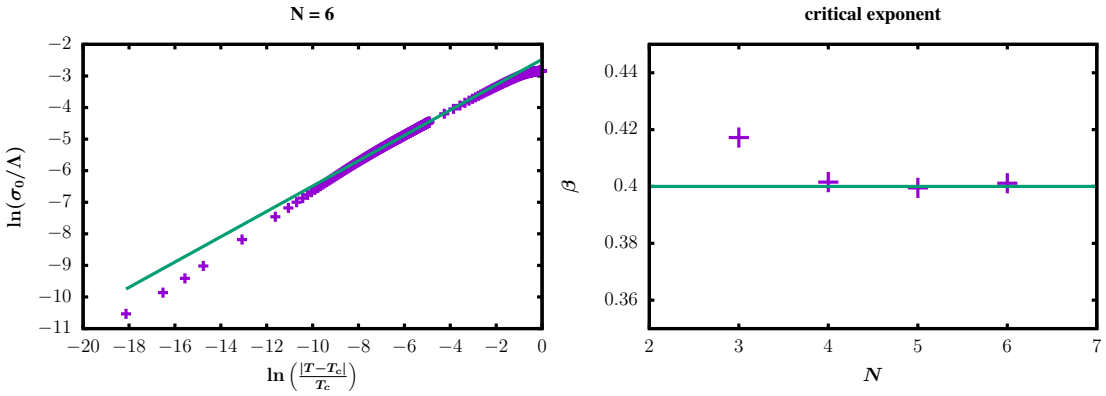

Figure 6: The left figure shows $\ln\left(\frac{\sigma_0}{\Lambda}\right)$ plotted on $\ln\left(\frac{|T-T_c|}{T_c}\right)$ for the previous parameters $N = 6$ and $\Lambda = 1500$ MeV. A linear fit was applied to the x-values between -4 and -8. The right figure shows the resulting critical exponents β for the truncation orders 3–6.

8.3.2 Explicit Symmetry Breaking

Under explicit symmetry breaking, the same behaviour as in the chiral limit can be observed concerning the minimum σ_0 and b_2. An increasing temperature decreases the coefficients and therefore the particle masses reduce.

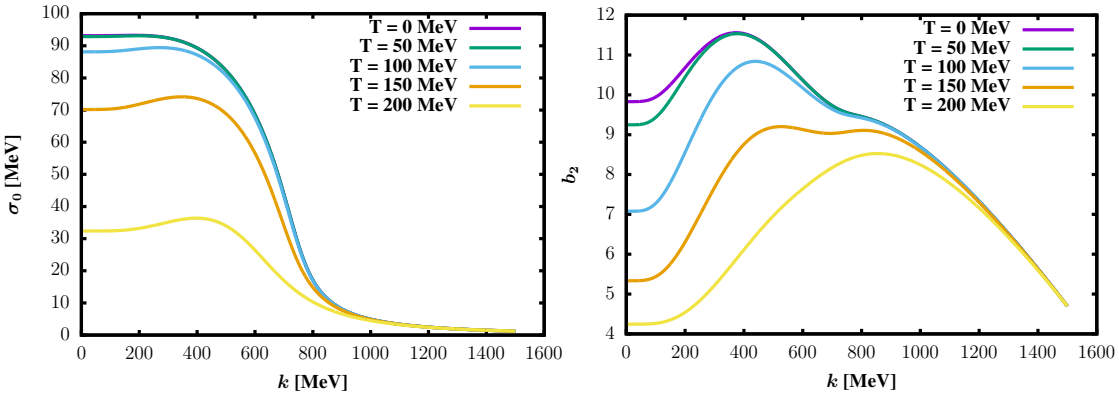

Figure 7: σ_0 and b_2 for explicit symmetry breaking, $\Lambda = 1500$ MeV and $N = 6$ at different temperatures.

Since the chiral symmetry is broken permanently, the order parameter can not exactly reach 0 at a finite temperature. The transition is washed out (cf. fig. 8), but one finds a pseudocritical temperature where the slope of the curve starts to reduce. Hence, here we also have a second order phase transition.

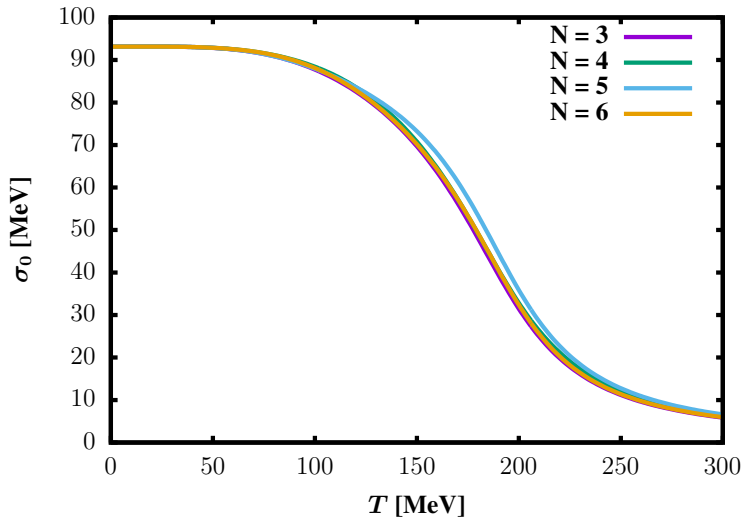

Figure 8: $\sigma_{0,k=0}$ for temperatures up to 300 MeV and the truncation orders 3–6. The UV cutoff is $\Lambda = 1500$ MeV.

8.4 Evolution for Non-Vanishing Chemical Potential

If we compute the critical temperature for several chemical potentials, we can draw a phase diagram for the QM model. In figure 9, this has been done for the chiral limit as well as for explicit symmetry breaking. Both lines belong to a second order phase transition, but the critical temperature of the explicitly broken phase is about 30 MeV higher. Both curves stop at a critical endpoint (CEP). The numerics do not find a critical temperature anymore. The critical temperature of both CEP is near 75 MeV. Other results suggest lower temperatures (between 50 and 60 MeV in the chiral limit) [10]. Possibly, the numerics being used here are not suited to get close enough to the CEP. Evidently, another phase transition happens beyond these points. According to grid simulations, the second order phase transition at the explicitly broken symmetry slowly turns into a crossover, whereas it suddenly becomes a first order phase transition in the chiral limit [10]. In a first order phase transition, the order parameter jumps to another value. This implies that there is a second (local) minimum which has now become the global minimum. Since the Taylor expansion in this work approximates the potential around one certain minimum, it becomes clear that a correct description of a first order phase transition is not possible.

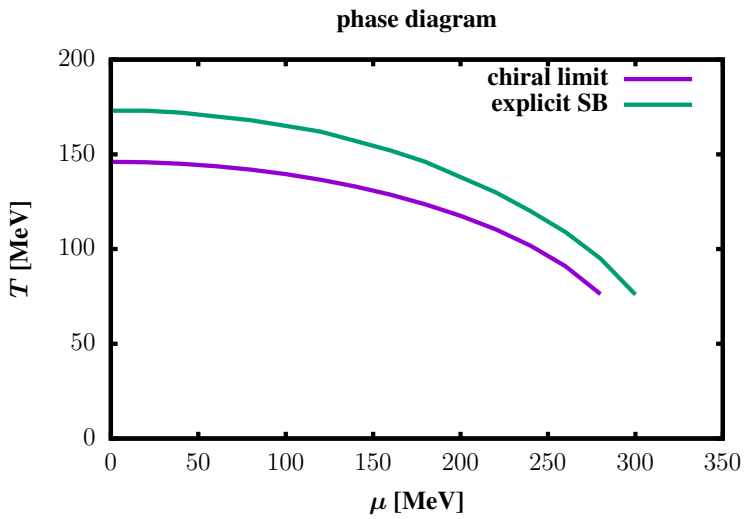

Figure 9: Critical temperatures plotted on the chemical potentials for $\Lambda = 1500$ MeV and $N = 6$ in the chiral limit (red) and for explicit symmetry breaking (green).

8.5 Pressure

Finally, the pressure of the system shall be examined. The grand canonical potential J obeys the thermodynamic relation for homogeneous systems

$$J = -PV = -T \ln Z. \tag{110}$$

Considering that $\ln Z = W = -\Gamma$ (without external sources), we can use the operator expansion of the effective (average) action (46) to find

$$P = -\frac{1}{\beta V} \int \mathrm{d}^4 x \, \Omega = -\Omega, \tag{111}$$

when $\Omega = \Omega_k^{(0)}(\sigma_0^2) = b_0$. We will use explicit symmetry breaking and set the vacuum pressure ($T = 0$, $\mu = 0$) to zero. Then the pressure is

$$P = \Omega_k^{(0)}(\sigma_0^2, \mu = 0, T = 0) - \Omega_k^{(0)}(\sigma_0^2, \mu, T). \tag{112}$$

Figure 10 shows the scaled pressure P/T^4 for several chemical potentials. At high temperatures, the scaled pressure decreases, which can be attributed to the finite UV cutoff. Studies including gluon degrees of freedom show a continuous increase in scaled pressure [5].

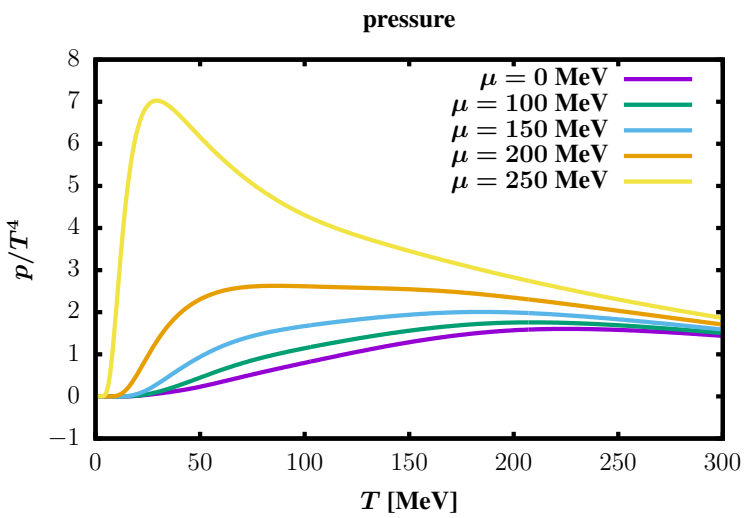

Figure 10: Temperature dependency of the scaled pressure P/T^4 for different chemical potentials, $\Lambda = 1500$ MeV and $N = 6$.

9 Summary

The target of this work was to study the application of renormalization group methods to (low-energy) QCD based on the example of the quark-meson model, where phase transitions could be observed. As a starting point, the functional renormalization group was introduced. Building upon the basic RG ideas, an approximation to the FRG, the proper-time renormalization group, was deduced. In what follows, the quark-meson model was introduced and the application of the PTRG to it was outlined. A flow equation was obtained, which was first analytically treated in a Taylor expansion. The resulting set of ordinary differential equations was computed numerically and the results were compared to prior expectations. Concerning the critical behaviour, we have seen that the second order phase transitions in the chiral limit as well as for explicitly broken symmetry are well described by the theory. We have also seen the limitations of the method used in this work. A Taylor expansion is not suited to describe all possible phenomena, e.g. first order phase transitions. The UV cutoff and the theory we input also limit the parameter range where our results are reliable. This could explicitly be observed in the scaled pressure. Gluon fluctuations that are important at high temperatures are neglected in this theory. Another problem is the appropriate choice of initial values, which does, on the one hand, succeed for fixed final IR values. On the other hand, the derivation from the QCD action has not yet succeeded. Therefore, many of the results can not be seen as definite physical predictions for experimental outcomes. Nevertheless, the theory sets a very good framework for the investigation of the QCD phase diagram and the power of the renormalization group theory becomes evident.

References

[1] Holger Gies. Introduction to the Functional RG and Applications to Gauge Theories. arXiv:hep-ph/0611146v1, 2006.

[2] Franz Mandl and Graham Shaw. *Quantum Field Theory.* Wiley, second edition, 2010.

[3] Jürgen Berges, Nikolaos Tetradis, and Christof Wetterich. Non-Perturbative Renormalization Flow in Quantum Field Theory and Statistical Physics. *Phys.Rept.*, 363:223–386, 2002. arXiv:hep-ph/0005122v1.

[4] Sen-Ben Liao. On the Connection Between Momentum Cutoff and Operator Cutoff Regularizations. *Phys.Rev.*, D53:2020–2036, 1996. arXiv:hep-th/9501124v2.

[5] Jens Braun, Kai Schwenzer, and Hans-Jürgen Pirner. Linking the Quark Meson Model with QCD at High Temperature. *Phys.Rev.*, D70(085016), 2004. arXiv:hep-ph/0312277v2.

[6] Bernd-Jochen Schaefer and Jochen Wambach. Renormalization Group Approach towards the QCD Phase Diagram. *Phys.Part.Nucl.*, 39:1025–1032, 2008. arXiv:hep-ph/0611191v1.

[7] Matthias Puhr. Diplomarbeit. Karl-Franzens-Universität Graz, 2012.

[8] B. Friman, C. Höhne, J. Knoll, S. Leupold, J. Randrup, R. Rapp, and P. Senger, editors. *The CBM Physics Book — Compressed Baryonic Matter in Laboratory Experiments.* Springer, January 2011.

[9] Victor Guillemin. Elliptic Operators. http://math.mit.edu/ vwg/18965notes.pdf, 11.08.2014.

[10] Bernd-Jochen Schaefer and Jochen Wambach. The Phase Diagram of the Quark-Meson Model. *Nucl.Phys.*, A757:479–492, 2005. arXiv:nucl-th/0403039v2.

[11] Agustin Nieto. Evaluating Sums over the Matsubara Frequencies. *Comput. Phys. Commun.*, 92(54), 1995. arXiv:hep-ph/9311210v1.

[12] William H. Press, Saul A. Teukolski, William T. Vetterling, and Brian P. Flannery. *Numerical Recipes 3rd Edition: The Art of Scientific Computing.* Cambridge University Press, 2007.

[13] Bernd-Jochen Schaefer and Hans-Jürgen Pirner. Renormalization Group Flow and Equation of State of Quarks and Mesons. *Nucl.Phys.*, A660:439–474, 1999. arXiv:nucl-th/9903003.

[14] Rainer Storn and Kenneth Price. Differential Evolution – A Simple and Efficient Heuristic for Global Optimization over Continuous Spaces. *Journal of Global Optimization*, 11:341–359, 1997.

A Taylor Series Expansion of the PTRG Flow

The expansion terms of the PTRG flow equation (79) can get very large, thus it makes sense to split them into different functions and write down the derivations of them separately. For a computer, this is just as easy to handle and higher truncation orders would easily be added. First, let us define the bosonic and fermionic threshold functions

$$\begin{aligned} B(E,T) &:= \coth\left(\frac{E}{2T}\right) \\ F(E,T,\mu) &:= \tanh\left(\frac{E-\mu}{2T}\right). \end{aligned} \tag{113}$$

If we define the short form

$$A(f(E),E) := \frac{1}{E} f(E), \tag{114}$$

the PTRG flow equation can be written as

$$\begin{aligned} \partial_t \Omega_k = \frac{k^5}{12\pi^2} \{ & A(B(E_\sigma,T),E_\sigma) + 3\, A(B(E_\pi,T),E_\pi) \\ & -2N_\mathrm{c}N_\mathrm{f}\, A(F(E_q,T,\mu)+F(E_q,T,-\mu),E_q)\}\,. \end{aligned} \tag{115}$$

With $A^{(j)} := \mathrm{d}^j A/(\mathrm{d}\sigma^2)^j$, a Taylor expansion takes the form

$$\begin{aligned} \partial_t \Omega_k^{(j)}(\sigma^2)\Big|_{\sigma=\sigma_0} = \frac{k^5}{12\pi^2} \Big\{ & A^{(j)}(B(E_\sigma,T),E_\sigma) + 3\, A^{(j)}(B(E_\pi,T),E_\pi) \\ & -2N_\mathrm{c}N_\mathrm{f}\, A^{(j)}(F(E_q,T,\mu)+F(E_q,T,-\mu),E_q)\Big\}\Big|_{\sigma=\sigma_0}. \end{aligned} \tag{116}$$

Let $f'(E) := \mathrm{d}f(E)/\mathrm{d}E$ and $E' := \mathrm{d}E/\mathrm{d}\sigma^2$. Then

$$A'(f(E),E) = \frac{f'E'}{E} - \frac{fE'}{E^2} \tag{117}$$

$$A''(f(E),E) = f\left(\frac{2E'^2}{E^3} - \frac{E''}{E^2}\right) + f'\left(\frac{E''}{E} - \frac{2E'^2}{E^2}\right) + \frac{f''E'^2}{E} \tag{118}$$

$$\begin{aligned} A'''(f(E),E) =& f\left(-\frac{6E'^3}{E^4} + \frac{6E'E''}{E^3} - \frac{E'''}{E^2}\right) + f'\left(\frac{6E'^3}{E^3} - \frac{6E'E''}{E^2} + \frac{E'''}{E}\right) \\ &+ f''\left(\frac{3E'E''}{E} - \frac{3E'^3}{E^2}\right) + \frac{f'''E'^3}{E} \end{aligned} \tag{119}$$

$$\begin{aligned} A^{(4)}(f(E),E) =& f\left(\frac{24E'^4}{E^5} - \frac{36E'^2E''}{E^4} + \frac{8E'E'''}{E^3} + \frac{6E''^2}{E^3} - \frac{E^{(4)}}{E^2}\right) \\ &+ f'\left(-\frac{24E'^4}{E^4} + \frac{36E'^2E''}{E^3} - \frac{8E'E'''}{E^2} - \frac{6E''^2}{E^2} + \frac{E^{(4)}}{E}\right) \\ &+ f''\left(\frac{12E'^4}{E^3} - \frac{18E'^2E''}{E^2} + \frac{4E'E'''}{E} + \frac{3E''^2}{E}\right) \\ &+ f'''\left(\frac{6E'^2E''}{E} - \frac{4E'^4}{E^2}\right) + \frac{f^{(4)}E'^4}{E} \end{aligned} \tag{120}$$

$$
\begin{aligned}
A^{(5)}(f(E),E) =& f\left(-\frac{120E'^5}{E^6}+\frac{240E'^3E''}{E^5}-\frac{60E'^2E'''}{E^4}-\frac{90E'E''^2}{E^4}\right.\\
&\left.+\frac{10E'E^{(4)}}{E^3}+\frac{20E''E'''}{E^3}-\frac{E^{(5)}}{E^2}\right)\\
&+f'\left(\frac{120E'^5}{E^5}-\frac{240E'^3E''}{E^4}+\frac{60E'^2E'''}{E^3}+\frac{90E'E''^2}{E^3}\right.\\
&\left.-\frac{10E'E^{(4)}}{E^2}-\frac{20E''E'''}{E^2}+\frac{E^{(5)}}{E}\right)\\
&+f''\left(-\frac{60E'^5}{E^4}+\frac{120E'^3E''}{E^3}-\frac{30E'^2E'''}{E^2}\right.\\
&\left.-\frac{45E'E''^2}{E^2}+\frac{5E'E^{(4)}}{E}+\frac{10E''E'''}{E}\right)\\
&+f'''\left(\frac{20E'^5}{E^3}-\frac{40E'^3E''}{E^2}+\frac{10E'^2E'''}{E}+\frac{15E'E''^2}{E}\right)\\
&+f^{(4)}\left(\frac{10E'^3E''}{E}-\frac{5E'^5}{E^2}\right)+\frac{f^{(5)}E'^5}{E}
\end{aligned}
\tag{121}
$$

$$
\begin{aligned}
A^{(6)}(f(E),E) =& f\left(\frac{720E'^6}{E^7} - \frac{1800E'^4E''}{E^6} + \frac{480E'^3E'''}{E^5} + \frac{1080E'^2E''^2}{E^5}\right.\\
&\left. -\frac{90E'^2E^{(4)}}{E^4} - \frac{360E'E''E'''}{E^4} - \frac{90E''^3}{E^4} + \frac{12E'E^{(5)}}{E^3}\right.\\
&\left. +\frac{30E''E^{(4)}}{E^3} + \frac{20E'''^2}{E^3} - \frac{E^{(6)}}{E^2}\right)\\
&+f'\left(-\frac{720E'^6}{E^6} + \frac{1800E'^4E''}{E^5} - \frac{480E'^3E'''}{E^4} - \frac{1080E'^2E''^2}{E^4}\right.\\
&\left. +\frac{90E'^2E^{(4)}}{E^3} + \frac{360E'E''E'''}{E^3} + \frac{90E''^3}{E^3} - \frac{12E'E^{(5)}}{E^2}\right.\\
&\left. -\frac{30E''E^{(4)}}{E^2} - \frac{20E'''^2}{E^2} + \frac{E^{(6)}}{E}\right)\\
&+f''\left(\frac{360E'^6}{E^5} - \frac{900E'^4E''}{E^4} + \frac{240E'^3E'''}{E^3} + \frac{540E'^2E''^2}{E^3} - \frac{45E'^2E^{(4)}}{E^2}\right.\\
&\left. -\frac{180E'E''E'''}{E^2} - \frac{45E''^3}{E^2} + \frac{6E'E^{(5)}}{E} + \frac{15E''E^{(4)}}{E} + \frac{10E'''^2}{E}\right)\\
&+f'''\left(-\frac{120E'^6}{E^4} + \frac{300E'^4E''}{E^3} - \frac{80E'^3E'''}{E^2} - \frac{180E'^2E''^2}{E^2}\right.\\
&\left. +\frac{15E'^2E^{(4)}}{E} + \frac{60E'E''E'''}{E} + \frac{15E''^3}{E}\right)\\
&+f^{(4)}\left(\frac{30E'^6}{E^3} - \frac{75E'^4E''}{E^2} + \frac{20E'^3E'''}{E} + \frac{45E'^2E''^2}{E}\right)\\
&+f^{(5)}\left(\frac{15E'^4E''}{E} - \frac{6E'^6}{E^2}\right) + \frac{f^{(6)}E'^6}{E}
\end{aligned}
\tag{122}
$$

Fortunately, the derivations of $F(E)$ and $B(E)$ are quite similar, which enables us to write

$$f'(E) = \frac{1}{2T}(1 - f(E)^2) \tag{123}$$

$$f''(E) := -\frac{f(E) - f(E)^3}{2T^2} \tag{124}$$

$$f'''(E) = -\frac{1}{4T^3}(3f(E)^4 - 4f(E)^2 + 1) \tag{125}$$

$$f^{(4)}(E) = -\frac{1}{2T^4}(-3f(E)^5 + 5f(E)^3 - 2f(E)) \tag{126}$$

$$f^{(5)}(E) = -\frac{1}{4T^5}(15f(E)^6 - 30f(E)^4 + 17f(E)^2 - 2) \tag{127}$$

$$f^{(6)}(E) = -\frac{1}{4T^6}(-45f(E)^7 + 105f(E)^5 - 77f(E)^3 + 17f(E)) \tag{128}$$

The energies are given in (80). From now on, $E_{x,0}^{(j)} := \mathrm{d}^j E_x/(\mathrm{d}\sigma^2)^j|_{\sigma=\sigma_0}$. The energies and their derivations, evaluated at the expansion point, are now listed. They can be

inserted into the above equations for the full Taylor series:

$$E_{\pi,0} = \sqrt{2\Omega' + k^2} \tag{129}$$

$$E'_{\pi,0} = \frac{\Omega''}{E_{\pi,0}} \tag{130}$$

$$E''_{\pi,0} = \frac{\Omega'''}{E_{\pi,0}} - \frac{\Omega''^2}{E^3_{\pi,0}} \tag{131}$$

$$E'''_{\pi,0} = \frac{3\Omega''^3}{E^5_{\pi,0}} - \frac{3\Omega''\Omega'''}{E^3_{\pi,0}} + \frac{\Omega^{(4)}}{E_{\pi,0}} \tag{132}$$

$$E^{(4)}_{\pi,0} = -\frac{15\Omega''^4}{E^7_{\pi,0}} + \frac{18\Omega''^2\Omega'''}{E^5_{\pi,0}} - \frac{4\Omega''\Omega^{(4)}}{E^3_{\pi,0}} - \frac{3\Omega'''^2}{E^3_{\pi,0}} + \frac{\Omega^{(5)}}{E_{\pi,0}} \tag{133}$$

$$\begin{aligned} E^{(5)}_{\pi,0} = {} & \frac{105\Omega''^5}{E^9_{\pi,0}} - \frac{150\Omega''^3\Omega'''}{E^7_{\pi,0}} + \frac{30\Omega''^2\Omega^{(4)}}{E^5_{\pi,0}} + \frac{45\Omega''\Omega'''^2}{E^5_{\pi,0}} \\ & - \frac{5\Omega''\Omega^{(5)}}{E^3_{\pi,0}} - \frac{10\Omega'''\Omega^{(4)}}{E^3_{\pi,0}} + \frac{\Omega^{(6)}}{E_{\pi,0}} \end{aligned} \tag{134}$$

$$\begin{aligned} E^{(6)}_{\pi,0} = {} & -\frac{945\Omega''^6}{E^{11}_{\pi,0}} + \frac{1575\Omega''^4\Omega'''}{E^9_{\pi,0}} - \frac{300\Omega''^3\Omega^{(4)}}{E^7_{\pi,0}} - \frac{675\Omega''^2\Omega'''^2}{E^7_{\pi,0}} + \frac{45\Omega''^2\Omega^{(5)}}{E^5_{\pi,0}} \\ & + \frac{180\Omega''\Omega'''\Omega^{(4)}}{E^5_{\pi,0}} + \frac{45\Omega'''^3}{E^5_{\pi,0}} - \frac{6\Omega''\Omega^{(6)}}{E^3_{\pi,0}} - \frac{15\Omega'''\Omega^{(5)}}{E^3_{\pi,0}} - \frac{10{\Omega^{(4)}}^2}{E^3_{\pi,0}} + \frac{\Omega^{(7)}}{E_{\pi,0}} \end{aligned} \tag{135}$$

$\Omega^{(j)}$ here denotes $\Omega^{(j)}_k(\sigma_0^2) = b_j$. Of course, in the chiral limit, all b_j are substituted by a_j. The sigma energies are

$$E_{\sigma,0} = \sqrt{k^2 + 2p_1} \tag{136}$$

$$E'_{\sigma,0} = \frac{p_2}{E_{\sigma,0}} \tag{137}$$

$$E''_{\sigma,0} = \frac{p_3}{E_{\sigma,0}} - \frac{p_2^2}{E^3_{\sigma,0}} \tag{138}$$

$$E'''_{\sigma,0} = \frac{3p_2^3}{E^5_{\sigma,0}} - \frac{3p_2p_3}{E^3_{\sigma,0}} + \frac{p_4}{E_{\sigma,0}} \tag{139}$$

$$E^{(4)}_{\sigma,0} = -\frac{15p_2^4}{E^7_{\sigma,0}} + \frac{18p_2^2p_3}{E^5_{\sigma,0}} - \frac{4p_2p_4}{E^3_{\sigma,0}} - \frac{3p_3^2}{E^3_{\sigma,0}} + \frac{p_5}{E_{\sigma,0}} \tag{140}$$

$$E^{(5)}_{\sigma,0} = \frac{105p_2^5}{E^9_{\sigma,0}} - \frac{150p_2^3p_3}{E^7_{\sigma,0}} + \frac{30p_2^2p_4}{E^5_{\sigma,0}} + \frac{45p_2p_3^2}{E^5_{\sigma,0}} - \frac{5p_2p_5}{E^3_{\sigma,0}} - \frac{10p_3p_4}{E^3_{\sigma,0}} + \frac{p_6}{E_{\sigma,0}} \tag{141}$$

$$\begin{aligned} E^{(6)}_{\sigma,0} = {} & -\frac{945p_2^6}{E^{11}_{\sigma,0}} + \frac{1575p_2^4p_3}{E^9_{\sigma,0}} - \frac{300p_2^3p_4}{E^7_{\sigma,0}} - \frac{675p_2^2p_3^2}{E^7_{\sigma,0}} + \frac{45p_2^2p_5}{E^5_{\sigma,0}} + \frac{180p_2p_3p_4}{E^5_{\sigma,0}} \\ & + \frac{45p_3^3}{E^5_{\sigma,0}} - \frac{6p_2p_6}{E^3_{\sigma,0}} - \frac{15p_3p_5}{E^3_{\sigma,0}} - \frac{10p_4^2}{E^3_{\sigma,0}} + \frac{p_7}{E_{\sigma,0}}, \end{aligned} \tag{142}$$

where $p_i := (2i-1)\, b_i + 2\,\sigma_0^2\, b_{i+1}$. Lastly, the quark energies are

$$E_{q,0} = \sqrt{k^2 + g^2\sigma_0^2} \tag{143}$$

$$E'_{q,0} = \frac{g^2}{2E_{q,0}} \tag{144}$$

$$E''_{q,0} = -\frac{g^4}{4E_{q,0}^3} \tag{145}$$

$$E'''_{q,0} = \frac{3g^6}{8E_{q,0}^5} \tag{146}$$

$$E^{(4)}_{q,0} = -\frac{15g^8}{16E_{q,0}^7} \tag{147}$$

$$E^{(5)}_{q,0} = \frac{105g^{10}}{32E_{q,0}^9} \tag{148}$$

$$E^{(6)}_{q,0} = -\frac{945g^{12}}{64E_{q,0}^{11}} \tag{149}$$

Selbstständigkeitserklärung

Hiermit versichere ich, die vorgelegte Thesis selbstständig und ohne unerlaubte fremde Hilfe und nur mit den Hilfen angefertigt zu haben, die ich in der Thesis angegeben habe. Alle Textstellen, die wörtlich oder sinngemäß aus veröffentlichten Schriften entnommen sind, und alle Angaben die auf mündlichen Auskünften beruhen, sind als solche kenntlich gemacht. Bei den von mir durchgeführten und in der Thesis erwähnten Untersuchungen habe ich die Grundsätze gute wissenschaftlicher Praxis, wie sie in der ‚Satzung der Justus-Liebig-Universität zur Sicherung guter wissenschaftlicher Praxis' niedergelegt sind, eingehalten. Gemäß § 25 Abs. 6 der Allgemeinen Bestimmungen für modularisierte Studiengänge dulde ich eine Überprüfung der Thesis mittels Anti-Plagiatssoftware.

Datum	Unterschrift